AD_____

Award Number: DAMD17-00-1-0444

TITLE: Integrating Organ Motion and Setup Uncertainty into
        Optimization of Modulated Electron Beam Treatment of
        Breast Cancer

PRINCIPAL INVESTIGATOR: Todd A. Pawlicki, Ph.D.

CONTRACTING ORGANIZATION: Stanford University
                           Stanford, California   94305-5401

REPORT DATE: August 2001

TYPE OF REPORT: Annual Summary

PREPARED FOR: U.S. Army Medical Research and Materiel Command
               Fort Detrick, Maryland   21702-5012

DISTRIBUTION STATEMENT: Approved for Public Release;
                         Distribution Unlimited

1

REPORT DOCUMENTATION PAGE		*Form Approved* *OMB No. 074-0188*

Public reporting burden for this collection of information is estimated to average 1 hour per response, including the time for reviewing instructions, searching existing data sources, gathering and maintaining the data needed, and completing and reviewing this collection of information. Send comments regarding this burden estimate or any other aspect of this collection of information, including suggestions for reducing this burden to Washington Headquarters Services, Directorate for Information Operations and Reports, 1215 Jefferson Davis Highway, Suite 1204, Arlington, VA 22202-4302, and to the Office of Management and Budget, Paperwork Reduction Project (0704-0188), Washington, DC 20503

1. AGENCY USE ONLY (Leave blank)	2. REPORT DATE August 2002	3. REPORT TYPE AND DATES COVERED Annual Summary (1 Aug 00 – 31 Jul 01)

4. TITLE AND SUBTITLE Integrating Organ Motion and Setup Uncertainty into Optimization of Modulated Electron Beam Treatment of Breast Cancer	5. FUNDING NUMBERS DAMD17-00-1-0444

6. AUTHOR(S)
Todd A. Pawlicki, Ph.D.

7. PERFORMING ORGANIZATION NAME(S) AND ADDRESS(ES) Stanford University Stanford, California 94305-5401 E-Mail: tpaw@reyes.stanford.edu	8. PERFORMING ORGANIZATION REPORT NUMBER

9. SPONSORING / MONITORING AGENCY NAME(S) AND ADDRESS(ES) U.S. Army Medical Research and Materiel Command Fort Detrick, Maryland 21702-5012	10. SPONSORING / MONITORING AGENCY REPORT NUMBER

20020930 042

11. SUPPLEMENTARY NOTES

Report contains color.

12a. DISTRIBUTION / AVAILABILITY STATEMENT Approved for Public Release; Distribution Unlimited	12b. DISTRIBUTION CODE

13. ABSTRACT *(Maximum 200 Words)*

This project is to develop, implement, and evaluate models of organ motion and setup uncertainty for dose calculation of radiotherapy treatment of the breast. These models are applied to accurate dose calculation for breast treatment using energy- and intensity-modulated electron radiotherapy (MERT). The premise is that MERT treatments will deliver a more conformal dose to the breast while minimizing the dose to normal tissues over conventional photon techniques. We have completed the following tasks: (1) developed theoretical models of organ motion and setup uncertainty based on published data, and (2) implemented those models into a Monte Carlo dose calculation code. We have developed a model of organ motion that correlates the dose in a static computed tomography scan to the actual case of patient breathing. A Gaussian model has been developed to account for setup uncertainty due to the random nature of setup uncertainty in radiotherapy, which has been demonstrated in published literature. These models have been implemented in a Monte Carlo code for radiotherapy dose calculations based on patient specific computed tomography scans. The successful completion of our goals now permits further study (specific aims 3 and 4) on the effect of these effects on MERT radiotherapy breast treatment.

14. SUBJECT TERMS breast cancer, organ motion and setup uncertainty, accurate dose calculation, radiotherapy, MERT, tomography scans			15. NUMBER OF PAGES 56
			16. PRICE CODE

17. SECURITY CLASSIFICATION OF REPORT Unclassified	18. SECURITY CLASSIFICATION OF THIS PAGE Unclassified	19. SECURITY CLASSIFICATION OF ABSTRACT Unclassified	20. LIMITATION OF ABSTRACT Unlimited

NSN 7540-01-280-5500

Standard Form 298 (Rev. 2-89)
Prescribed by ANSI Std. Z39-18
298-102

Table of Contents

Introduction

Energy- and intensity-modulated radiotherapy (MERT) is the optimization of many small beamlets of different energies and intensities to produce a highly conformal dose distribution. Each individual beamlet's dose distribution must be calculated in a computed tomography based representation of the patient. The relative weight of each beamlet is optimized using a computer implemented mathematical technique. When the optimized beamlet weights are applied to the patient, a conformal dose distribution is achieved. This is called inverse planning and produces very conformal dose distributions when coupled with MERT. When applied to radiotherapy breast treatment, MERT dose distributions conform to the treated breast while, at the same time, spares the lung, heart, and contralateral breast to excessive irradiation. Two effects that thwart MERT treatments are, inaccurate dose calculation, and the effects of patient organ motion and daily setup uncertainty. The overall aim of this project is to use accurate Monte Carlo dose calculation as the basis for the development and implementation of mathematical models of both organ motion and setup uncertainty. Monte Carlo is generally accepted by the medical physics community as the most accurate dose calculation model available. Once Monte Carlo is combined with realistic models of organ motion and setup uncertainty, we can include those effects into the calculation of beamlets for optimization. Models of organ motion and setup uncertainty are developed, implemented, and experimentally tested, so we can study the improvement in the MERT dose distributions when these deleterious effects associated with radiotherapy treatment are included in the beamlet calculation and optimization processes. The successful completion of this project will facilitate the implementation of MERT as a realistic clinical option for breast cancer treatment. All patient-related factors should be included in the dose calculation and optimization processes to obtain clinically realistic dose uniformity in the target volume and normal tissue sparing. We believe that that the inclusion of organ motion and setup uncertainty into accurate Monte Carlo dose calculations will significantly improve optimized MERT treatment plans. The degree of improvement in the final treatment plan when organ motion and setup uncertainty are included in the dose calculation of beamlets for the optimization process can now be investigated after the successful completion of our specific aims for the first year of research.

Body

Traditional radiotherapy treatment for breast cancer consists of two tangential photon beams. The tangential beam configuration is used to limit the dose to the lung (and heart for left breast treatment) by limiting the beam divergence into these normal tissues. However, even with this approach, conventional radiotherapy breast treatment is associated with unwanted radiation complications[1-6]. These include: high dose to the heart and lung (resulting in radiation pericarditis and radiation pneumonitis), increased radiation scatter to the untreated breast (resulting in an increased risk of secondary cancer), and poor cosmetic results for patients with larger breasts. A novel approach using electron beams, rather than photon beams, has been proposed to overcome these problems[7]. In this technique, a conventional broad electron beam (25x25 cm^2) is subdivided into many small electron beams (1x1 cm^2), called beamlets. Each beamlet can then be subject to energy- and intensity modulation. This is done by initially calculating the dose distribution for each beamlet of different electron beam energies in the patient. Then, a computer implemented optimization algorithm is applied to each beamlet in order to determine the optimal intensity for each beamlet energy. The result is a highly conformal dose distribution to the treated breast with minimal dose to adjacent normal tissues. This approach is called energy- and intensity modulated radiotherapy (MERT) and is a technique called inverse planning. It is the physical characteristics of electron beams that give MERT a real advantage over photon beams in treating breast cancer with radiation. Until recently, various theoretical and technical limitations have not allowed the clinical fruition the dosimetrically advantageous MERT treatments. Some of these are currently being overcome with other DOD funded research[8,9]. Additional theoretical limitations, which are the subject of this research, is the organ motion and daily setup uncertainty associated with radiotherapy breast cancer treatment. By including the effects of organ motion and setup uncertainty into accurate Monte Carlo beamlet calculations for the optimization algorithm, we will ensure that beamlets calculated for MERT will be optimized for a clinically real situation and thus, the planned and delivered doses will be the same. Current techniques to account for organ motion and setup uncertainty is to simply ignore them altogether or to add a large margin around the treated volume. An increase in margin, however, results in an increase in the volume of normal tissue irradiated, which in turn, increases normal tissue complications. The MERT technique will be a very promising modality for breast cancer treatment provided all clinical circumstances are accounted for in the planning/dose calculation process. The successful completion of the project will help the clinical realization of MERT to improve the target dose uniformity and

5

conformity and reduce dose to the lung, heart and contralateral breast.

This project has 4 specific aims: (1) develop theoretical models of organ motion and setup uncertainty, (2) implement the models into Monte Carlo dose calculations, (3) verification of the new Monte Carlo programs, and (4) evaluate MERT treatment plans for 10 breast cancer cases. We report on the research accomplishments associated with the tasks outlined in the approved "Statement of Work" below for our research between August 1, 2000 and July 31 2001.

1. The Monte Carlo dose calculation code system

We have developed a general purpose Monte Carlo EGS4[10] user code MCDOSE[11] that can be used for patient specific electron dose calculations. Excellent agreement was achieved between the MCDOSE results and measurements[12] and the well benchmarked EGS4/BEAM/DOSXYZ code[13]. Our Monte Carlo code system includes the option to produce beamlets for both photon and electron treatment optimization. The requirement of dose calculation accuracy for truly optimized treatment plans has been demonstrated and is shown in Figure 1. Calculation inaccuracies have also been demonstrated with inverse planning for photon beams[14]. The code system has also been developed and demonstrated to produce beamlet dose calculations for MERT optimized breast treatment plans[15].

2. Computer model of organ motion

Tumor motion due to respiration during radiation treatment will lead to "motion artifacts" in dose distributions. Intra-fraction organ motion creates a broadened dose penumbra, which limits the conformal dose coverage to the tumor. We have developed analytical models to trace the motion of the tumor in lung based on the initial patient computed tomography data and the motion data measured during a radiotherapy breast treatment. This allows the reconstruction of realistic dose distributions received by the patient during a fraction of treatment. The patient geometry at any time during a breathing cycle is reconstructed using the computed tomography data taken at the inspiration and expiration phases and the chest wall motion measured using an optical motion detector. Accurate correlation between the voxels in the inspiration (or expiration) geometry and the voxels in the reconstructed geometry at any point of the breathing cycle is established so that the dose to a voxel (or an organ) can be accumulated accurately during a treatment[16,17].

3. Computer model of setup uncertainty

The intra-fraction setup uncertainty is a random phenomena[18,19] having a Gaussian distribution. The variance of the Gaussian distribution is different for each translational axis (see Figure 2) and depends on the anatomical region being treated. We used a "real-time" method to incorporate setup uncertainty into our Monte Carlo calculations. This was done by perturbing the incident particles before they enter the patient. The perturbation was done by sampling from three individual Gaussian distributions, one for each translational x, y or z axis in the patient (i.e., Anterior-Posterior, Right-Left and Superior-Inferior). The variance of the each Gaussian distribution was obtained from the literature[19] and is in the process of being verified by measurement in our department. Setup uncetainty was assumed to consist of x, y and z translations that are independent. The model is shown schematically in Figure 3. Our approach to include setup uncertainty is different than a simple Gaussian smoothing after the dose has been calcualated. The "real-time" perturbation of each incident particle before it enters the patient ensure that each particle that enters the patient "sees" the correct source-to-surface distance and heterogeneities within the patient. For a Gaussian smooting, after the dose calculation is completed, dose near heterogeneities is considered in only an approximate way. Ongoing work for this project is to compare our method with the Gaussian smoothing method of the static dose distribution for any differences in the results.

4. Implementation and effects of organ motion

The method has been implemented for Monte Carlo treatment planning by interfacing with the MCDOSE code. MCDOSE phantom files for different phases of the breathing cycle were generated and the 3D dose data were obtained from MCDOSE simulations. The final dose distribution was reconstructed from these 3D dose data. The purpose of this work was to compare the effects of organ motion, specifically thoracic movement on conventional photon and modulated electron beam dose distribution. The Monte Carlo MCDOSE treatment planning system was used for this study to investigate breast treatment using parallel opposed 6MV tangential beams and MERT. The MERT treatment consisted of applying multiple beams consisting of 6, 9, 12, 16, 20 MeV energies to conform the prescription dose to the target. For the patient computed tomography scans used for initial treatment planning, the dose was normalized to 50 Gy. Two more computed tomography slices were generated simulating patient exhalation and inhalation. Treatment planning was done on all three images using the same parameters.

There was not a significant change in dose to the target with simulated motion of one cm posteriorly and anteriorly with respect to the original patient computed tomography scan. MERT showed an improvement in conformity of overall dose to the target as well as avoiding dose to the lung. For photon beam treatment the right lung beneath the target breast shows a disparity in absolute dose and the volume of tissue irradiated at different phases of the breathing cycle. During exhalation 7% of the right lung volume received a dose of 17.5 Gy while at inhalation 7% of the right lung volume received a dose of 35.5 Gy. At mid-plane between the two extremes of the cycle only 2% of the right lung received a dose of 35.5 Gy. For MERT, the lung dose remained negligible, however, there was an increase in lung dose during inhalation. Ten percent of the lung received a dose of 5 Gy, which was a dose increase of 5% from the median plane of breathing cycle. The maximum dose to the lung during inspiration was 87% of the prescription dose while at median phase of the breathing cycle the maximum dose decreased to 80% of the prescription dose and at expiration this dose was less than 6% of the prescribed dose when using photon beams.

5. Implementation and effects of setup uncertainty

Results obtained using our approach to include setup uncertainty in Monte Carlo IMRT dose calculations was demonstrated for a clinical photon beam inverse planning case. We present a case for the treatment of a metastatic lesion at T11 - T12. This patient was planned with 9 coplanar intensity modulated fields of 15 MV photons. Figure 4 shows the axial dose distribution for Monte Carlo calculations with and without setup uncertainty for the first clinical case. In general, the dose results look similar. However, there is a subtle difference in target coverage and slightly larger difference in spinal cord dose. The difference in the two dose distributions (with and without setup uncertainty) is made clear by plotting the cummulative dose volumes histograms as shown in Figure 5. There is similar target coverage but an increased dose was delivered to adjacent tissues including the spinal cord. Other critical structures are distant to the target and the DVHs with and without setup uncertainty are deemed to be clinically the same. It is also worth noting that the DVH to the entire patient's body (skin) are the same for both cases so the total energy deposited in the patient is the same for our simulations with and without setup uncertainty. The dose is simply spread over a large volume to other tissues.

A second case was treated for a lesion in the thorax and planned with 5 inverse planned coplanar fields of 4 MV photons. An interesting aspect is demonstrated in the case shown in Figures 6 and 7. Figure 6 shows an axial dose distribution for Monte Carlo calculations with and with out setup uncertainty for the second clinical case. In Figure 7, the target DVHs for the second clinical case show a slight increase in target dose homogeneity when setup uncertainty is considered in the IMRT dose calculation. We believe the reason for this is that the hot-spots within the target will be smoothed away. It is worth noting that IMRT treatment plans typically have a large dose gradient across the target volume. The gradient can be upwards of 30% in some cases. Setup uncertainty then, will smooth these high dose regions and provide a more homogeneous dose to the target. However, this smoothing will come at the expense of an increased dose to adjacent critical structures. The amount of that dose increase may depend on the shape and location of the target. For critical structures distal to the target and in low dose regions, the effect of setup uncertainty is not large. The extent to which these effects are reduced when using MERT is being determined.

Similar to a simple Gaussian smoothing of the static dose distribution, our method is equivalent to including the effects of setup uncertainty over an infinite number of small fractions[20-22]. Our method of including the setup uncertainty implies that all the statistical fluctuations associated with setup uncertainty have been averaged out to the maximum possible extent. There may be cases with less differences and there may be cases with greater differences in the DVHs. We feel that by including setup uncertainty in our method at least gives the clinician a reasonable estimate of the possible effects of setup uncertainty during treatment. Additionally, our method does combine proper consideration of a patient's heterogeneities and irregular contours by accurate Monte Carlo dose calculation .

Key Research Accomplishments

- *Develop computer model for organ motion*: A model of organ motion has been developed. This model uses clinical computed tomography scan of actual breast cancer patients. Thus, the models are realistic estimates of patient positioning and immobilization.

- *Implement organ motion model into Monte Carlo code*: We have implemented the organ motion model into our Monte Carlo code called MCDOSE. This model is implemented in a general sense and can also be applied to conventional treatments as well as MERT treatments that are calculated with MCDOSE.

- *Develop computer model of setup uncertainty*: We have developed a model of setup uncertainty based on published data. Since it has been shown that setup uncertainty is a random process in radiotherapy, our model has been implemented based on the Gaussian distribution. The implementation allows the adjustment of the Gaussian parameters as the setup uncertainty measurements become more accurate in the future.

- *Implement setup uncertainty model into Monte Carlo code*: We have implemented our model of setup uncertainty in our MCDOSE Monte Carlo code. It has been implemented in such a way that it can be "turned-on" and "turned-off" for successive Monte Carlo calculations to investigate its effects on dose results and optimization.

- *Initial study of the effects of organ motion and setup uncertainty on optimization*: Our initial results show that the effects of setup uncertainty limit the degree of optimization of the dose distribution if setup uncertainty is not included in the beamlet simulation for optimization.

Reportable Outcomes

Peer-reviewed papers resulting from or supported in part by this grant:

- C.M. Ma, T. Pawlicki, M.C. Lee, S.B. Jiang, J.S. Li, J. Deng, E. Mok, B. Yi, G. Luxton and A.L. Boyer, Energy- and intensity-modulated electron beams for radiotherapy, Phys. Med. Biol. (2000) 45: 2293-2311

- J.S. Li, T. Pawlicki, J. Deng, S.B. Jiang, E. Mok and C.M. Ma, Validation of a Monte Carlo dose calculation tool for radiotherapy treatment planning, Phys. Med. Biol. (2000) 45: 2969-2985

- Pawlicki T, Jiang SB, Li JS, Deng J, Ma CM, Monte Carlo dose calculation and setup uncertainty, To be submitted to Med Phys, May 2002.

Meeting abstracts resulting from or supported in part by this grant:

- Ding M, Deng J, Li JS, Lee MC, Jolly J, Pawlicki T and Ma C-M, Investigation of dose correlation for organ motion, Accepted for oral presentation at the 43rd Annual Meeting of the American Association of Physicists in Medicine in Salt Lake City, Utah from July 22-26, 2001.

- Jolly J, Ding M, Pawlicki T, Chu J and Ma C-M, Monte Carlo simulation of the effect of thoracic motion on breast treatment, Accepted for oral presentation at the 43rd Annual Meeting of the American Association of Physicists in Medicine in Salt Lake City, Utah from July 22-26, 2001.

- Pawlicki T, T.M. Guerrero, S.B. Jiang, J. Deng, J. Li, A.L. Boyer and C.-M. Ma, The role of set-up uncertainty in intensity modulated treatment planning, Oral presetation at the 42nd Annual Meeting of the *American Society for Theraputic Radiology and Oncology*, Boston, MA, October 22 – October 26, 2000.

- Pawlicki T, Jiang SB, Li JS, Deng J and Ma C-M, Including setup uncertainty in Monte Carlo Dose Calculation for IMRT, Oral presentation at the 2000 World Congress on Medical Physics and Biomedical Engineering (in conjunction with the 42nd Annual Meeting of the *American Association of Physicists in Medicine*), Chicago, IL, July 23-28, 2000.

Funding applied for based on work resulting from or supported in part by this grant:

None

Conclusions

We have made significant progress during our first-year investigation. We have successfully performed the tasks scheduled in the "Statement of Work". We have developed models of organ motion and setup uncertainty for implementation into our MCDOSE Monte Carlo code and these models have been successfully implemented into that code. Preliminary results indicate that if organ motion and setup uncertainty are not included in the pre-optimization beamlet simulations, then the beamlet weights and subsequent dose distributions are not truly optimized. Further studies as scheduled in the "Statement of Work" are needed to complete the verification of our implementation and also to determine the degree of efficacy of MERT treatments for breast cancer. In the process of this work we have found that our models and implementation can be utilized to improve the conventional treatment of breast cancer as well.

References

1. Buchholtz TA, Gurgoze E, Bice WS and Prestidge BR (1997) Dosimetric analysis of intact breast irradiation in off-axis planes. *Int J Radiat Oncol Biol Phys* 39:261-7.

2. Gyenes G, Gagliardi G, Lax I, Fornader T and Rutqvist LE (1997) Evaluation of irradiated heart volumes in stage I breast cancer patients treated with postoperative adjuvant radiotherapy. *J Clinic Oncol* 15:1348-53.

3. Cazzaniga LF, Bossi A, Cosentino D, Frigerio M, Martinelli A, Monti A, Morresi A, Ostinelli A, Scandolaro L, Valli MC and Besana G (1998) Radiological findings when very small lung volumes are irradiated in breast and chest wall treatment. *Radiat Oncol Inves* 6:58-62.

4. Fraass BA, Roberson PL and Lichter AS (1985) Dose to the contralateral breast due to primary breast irradiation. *Int J Radiat Oncol Biol Phys.* 11:485-97.

5. Muller-Runkel R and Kalokhe UP (1990) Scatter dose from tangential breast irradiation to the uninvolved breast. *Radiology* 175:873-6.

6. Moody AM, Mayles WP, Bliss JM, A'Hern RP, Owen JR, Regan J, Broad B and Yarnold JR (1994) The influence of breast size on late radiation effects and association with radiotherapy dose inhomogeneity. *Radiot Oncol* 33:106-12.

7. Ma CM (proposal start date, October 1998) Energy- and intensity-modulated electron beams for breast cancer treatment. *U. S. Army Medical Research and Material Command Breast Cancer Research Program, proposal number BC971292.*

8. Jiang SB (project start date, March 2000) A multi-leaf collimator for modulated electron radiation therapy for breast cancer. *U. S. Army Medical Research and Material Command Breast Cancer Research Program, proposal number BC990213.*

9. Lee MC (project start date, July 2001) Beam delivery verification for modulated electron radiation therapy treatment of breast cancer. *U. S. Army Medical Research and Material Command Breast Cancer Research Program, proposal number BC000838.*

10. Nelson R, Hirayama H and Rogers DWO. (1985) *The EGS4 code system*, Stanford Linear Accelerator Center Report SLAC-265 (SLAC, Stanford, CA).

11. Ma, C-M; Li, JS, Pawlicki, T, Jiang, SB, and Deng, J (2002) MCDOSE – A Monte Carlo dose calculation tool for radiation therapy treatment planning. In Schlegel,W.; Bortfeld, T.; editors. Proceedings of the 13th International Conference on the Use of Computers in Radiation Therapy. Heidelberg, Germany: Springer:123-125.

12. Ma C-M, Mok E, Kapur A, Pawlicki T, Findley D, Brain S, Forster K and Boyer AL, (1999)

Clinical implementation of a Monte Carlo treatment planning system, *Med. Phys.* 26: 2133-43

13. Li JS, Pawlicki T, Deng J, Jiang SB, Mok E and Ma C-M, (2000) Validation of a Monte Carlo dose calculation tool for radiotherapy treatment planning, *Phys. Med. Biol.* 45: 2969-2985.

14. Pawlicki T, Guerrero TG, Jiang SB, Deng J, Li JS, Boyer AL and Ma C-M, "Monte Carlo dose calculation of clinical IMRT treatment plans," Submitted to Radiother and Oncol, March 2001.

15. Ma C-M, Pawlicki T, Lee MC, Jiang SB, Li JS, Deng J, Mok E, Yi B, Luxton G and Boyer AL, (2000) Energy- and intensity-modulated electron beams for radiotherapy, *Phys. Med. Biol.* 45: 2293-2311.

16. Ding M, Deng J, Li JS, Lee MC, Jolly J, Pawlicki T and Ma C-M (2001) Investigation of dose correlation for organ motion. Oral presentation at the 43rd Annual Meeting of the American Association of Physicists in Medicine in Salt Lake City, Utah from July 22-26.

17. Jolly J, Ding M, Pawlicki T, Chu J and Ma C-M, Monte Carlo simulation of the effect of thoracic motion on breast treatment. (2001) Oral presentation at the 43rd Annual Meeting of the American Association of Physicists in Medicine in Salt Lake City, Utah from July 22-26.

18. Samson MJ, van Sörnsen de Koste JR, de Boer HCJ, Tankink H, Verstraate M, Essers M, Visser AG and Senan S. (1999) An analysis of anatomic landmark mobility and setup deviations in radiotherapy for lung cancer. *Int. J. Radiat. Oncol. Biol. Phys.* 43:827-32.

19. Schewe JE, Balter JM, Lam KL and Ten Haken RK (1996) Measurement of patient setup errors using port films and a computer-aided graphical alignment tool. *Med. Dosim.* 21:97-104.

20. Killoran JH, Kooy HM, Gladstone DJ, Welte FJ and Beard CJ. (1997) A numerical simulation of organ motion and daily setup uncertainties: implications for radiation therapy. *Int. J. Radiat. Oncol. Biol. Phys.* 37:213-21.

21. Leong J (1987) Implementation of random positioning error in computerized radiation treament planning systems as a result of fractionation. *Phys. Med. Biol.* 32:327-34.

22. Lujan AE, Ten Haken RK, Larsen EW and Balter JM. (1999) Quantization of setup uncertainties in 3-D dose calculations. *Med. Phys.* 26:2397-2402.

Appendices

List of Figures quoted in the body of text:

Figure 1: These are two plans, one optimized based on FSPB beamlets and one based on Monte Carlo beamlets (a). All other parameters are held constant. The result is more conformal and homogeneous dose distribution to the target. The DVHs show better coverage and critical structure sparing (b). The solid line denotes the Monte Carlo dose calculation result and the dashed line denotes the conventional dose calculation result.
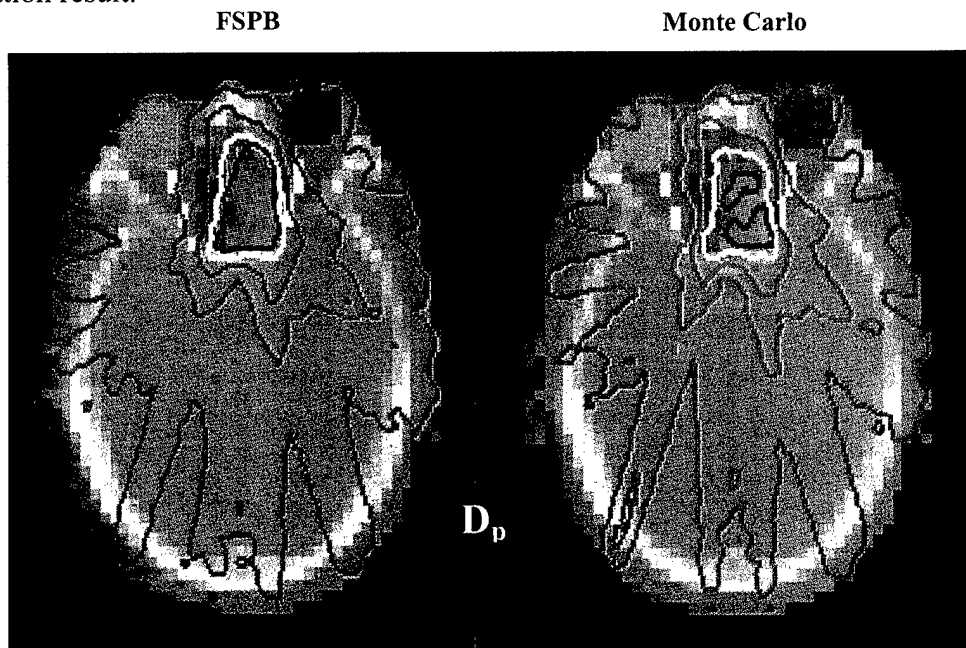
(a)
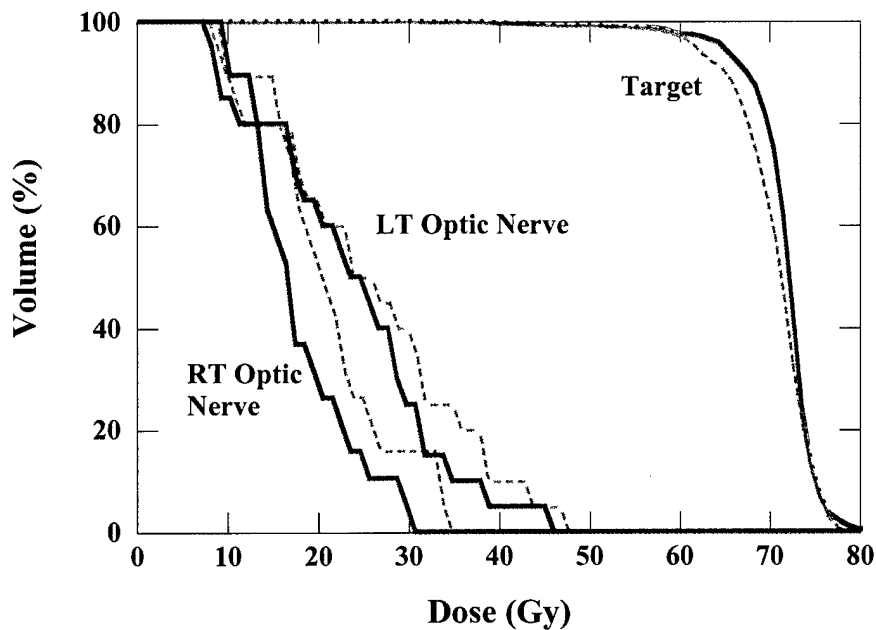
(b)

Figure 2: These are the Gaussian distributions for setup uncertainty as obtained from the literature for one specific treatment site. It should be noted that the distribution is different along the x, y and z principle axes. Also, these curves were generated using the subroutines from our Monte Carlo software so they serve as a quality assurance test of our code.
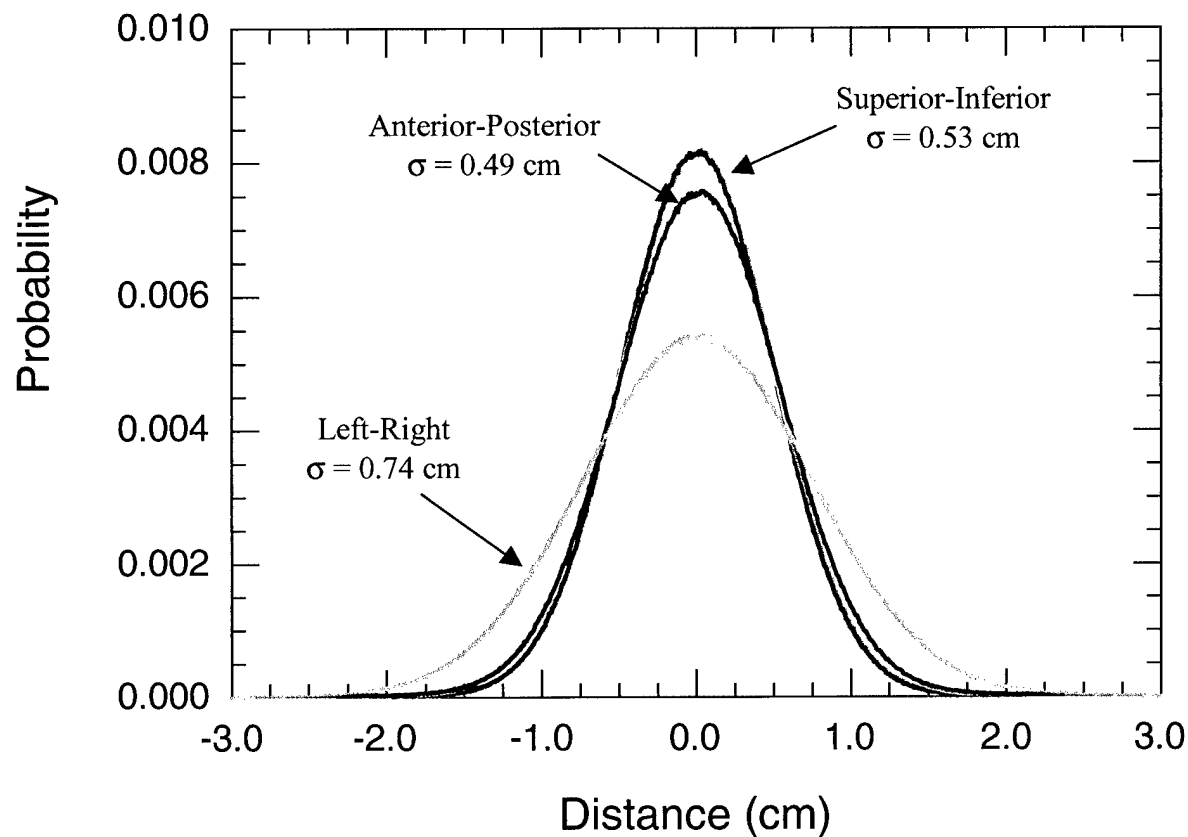
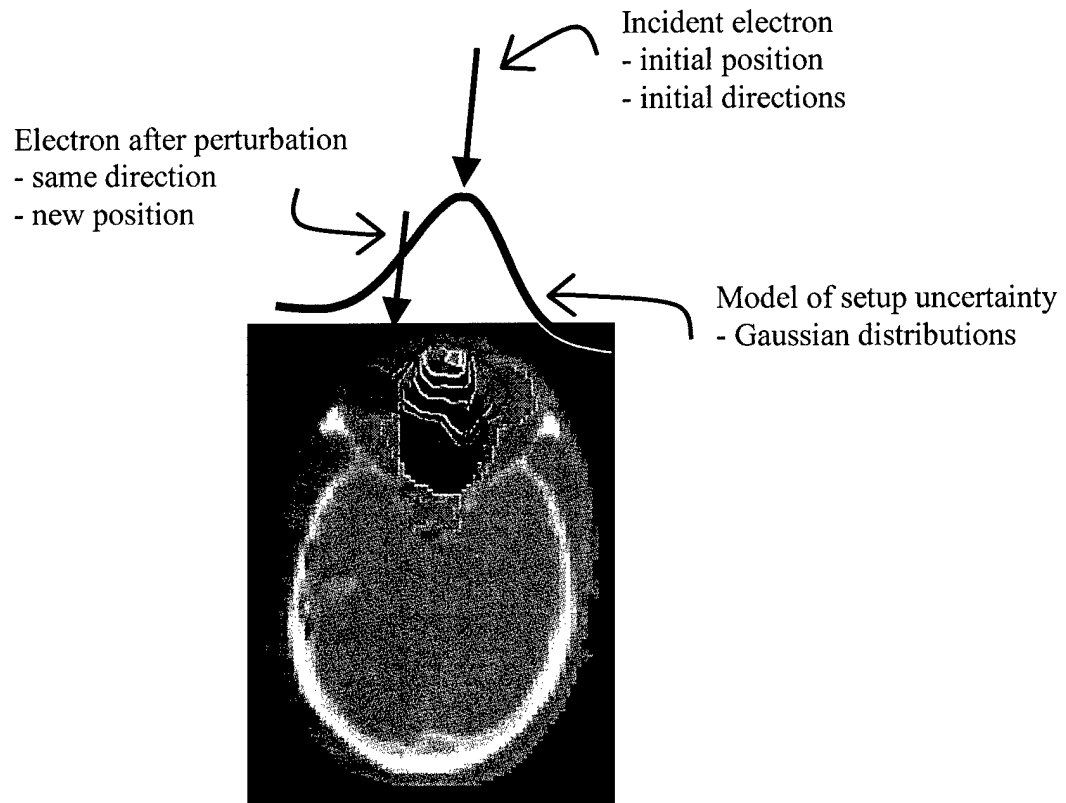Figure 3: This is a schematic of our implementation of setup uncertainty in our Monte Carlo dose calculation code.

Incident electron
- initial position
- initial directions

Electron after perturbation
- same direction
- new position
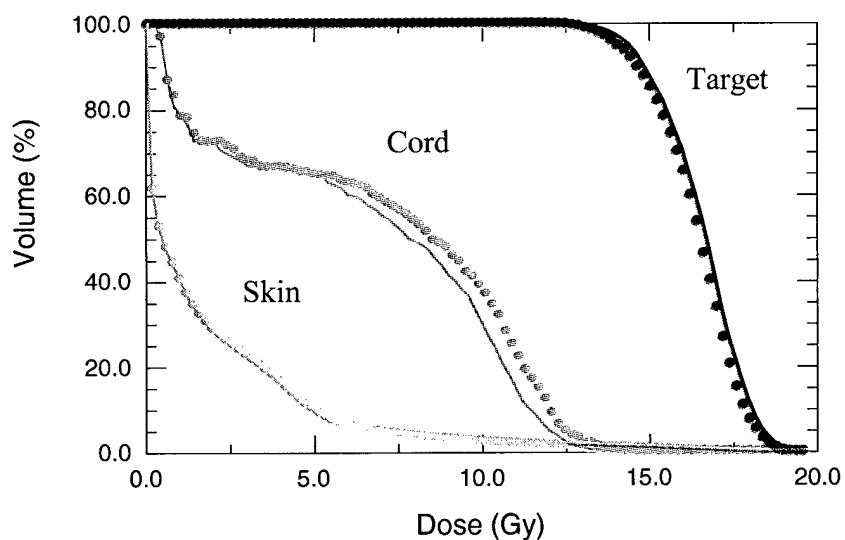
Model of setup uncertainty
- Gaussian distributions

Figure 4: Axial and sagittal computed tomography slice showing the Monte Carlo calculated IMRT dose distributions with (thick line) and without (thin line) setup uncertainty included. The target (metastatic lesion at T11-T12) is shown in green and the spinal cord in red.

4.9 Gy

18.1 Gy
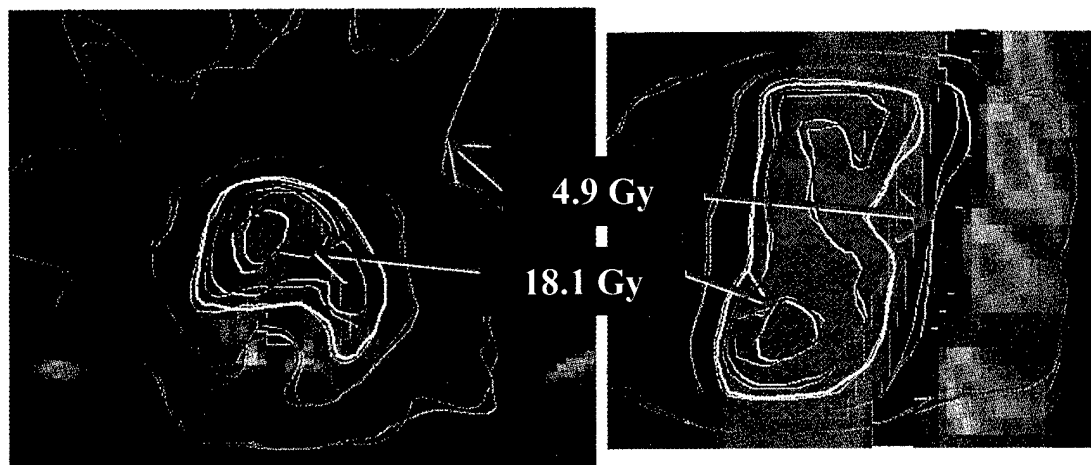
Figure 5: This is the dose-volume histogram of the dose distributions shown in Figure 4. There is an increase in dose to the spinal cord. The calculation with setup uncertainty is shown in by the curves with closed circles and without setup uncertainty by the solid line.

Figure 6: Axial and sagittal computed tomography slice showing the Monte Carlo calculated IMRT dose distributions with (thick line) and without (thin line) setup uncertainty included. The target is shown in green and the spinal cord in red.
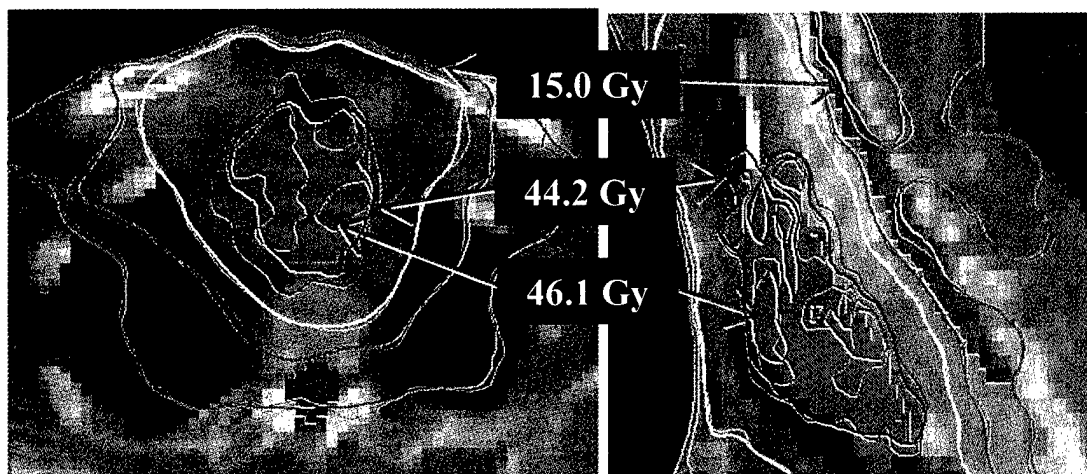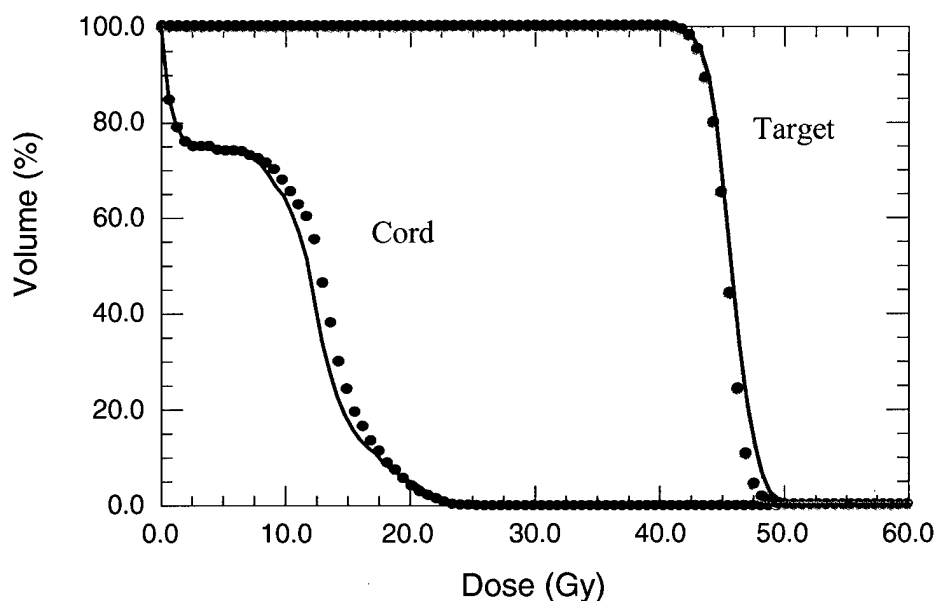

Figure 7: This is the dose-volume histogram of the dose distributions shown in Figure 6. Note the increase in target dose homogeneity. However, there is also a corresponding slight increase in dose to the spinal cord. The calculation with setup uncertainty is shown in by the curves with closed circles and without setup uncertainty by the solid line.

List of manuscripts submitted with this report

1. C.-M. Ma, T. Pawlicki, M.C. Lee, S.B. Jiang, J.S. Li, J. Deng, E. Mok, B. Yi, G. Luxton and A.L. Boyer (2000) Energy- and intensity-modulated electron beams for radiotherapy. *Phys. Med. Biol.* 45: 2293-2311.

2. J.S. Li, T. Pawlicki, J. Deng, S.B. Jiang, E. Mok and C.-M. Ma (2000) Validation of a Monte Carlo dose calculation tool for radiotherapy treatment planning. *Phys. Med. Biol.* 45: 2969-2985.

Energy and intensity modulated electron beams for radiotherapy

C-M Ma, T Pawlicki, M C Lee, S B Jiang, J S Li, J Deng, B Yi, E Mok and A L Boyer

Department of Radiation Oncology, Stanford University School of Medicine, Stanford, CA 94305-5304, USA

E-mail: cma@reyes.stanford.edu

Abstract. This work investigates the feasibility of optimizing energy- and intensity-modulated electron beams for radiation therapy. A multileaf collimator (MLC) specially designed for modulated electron radiotherapy (MERT) was investigated both experimentally and by Monte Carlo simulations. An inverse-planning system based on Monte Carlo dose calculations was developed to optimize electron beam energy and intensity to achieve dose conformity for target volumes near the surface. The results showed that an MLC with 5 mm leaf widths could produce complex field shapes for MERT. Electron intra- and inter-leaf leakage had negligible effects on the dose distributions delivered with the MLC, even at shallow depths. Focused leaf ends reduced the electron scattering contributions to the dose compared with straight leaf ends. As anticipated, moving the MLC position toward the patient surface reduced the penumbra significantly. There were significant differences in the beamlet distributions calculated by an analytic 3-D pencil beam algorithm and the Monte Carlo method. The Monte Carlo calculated beamlet distributions were essential to the accuracy of the MERT dose distribution in cases involving large air gaps, oblique incidence and heterogeneous treatment targets (at the tissue–bone and bone–lung interfaces). To demonstrate the potential of MERT for target dose coverage and normal tissue sparing for treatment of superficial targets, treatment plans for a hypothetical treatment were compared using photon beams and MERT.

(Some figures in this article are in colour only in the electronic version; see www.iop.org)

1. Introduction

Photon beams have been an effective modality for breast cancer treatment in radiation therapy. Although such conventional treatment with tangential photon fields has been successful, the following two problems (or potential areas of improvement) remain:

(a) The inclusion of the lung and other normal tissues, and sometimes of a small volume of the heart, in the high-dose volume due to tumour location, patient size or in the case of chest-wall treatments.

(b) High exit or scatter dose to the normal structures such as the lung, the heart and the contralateral breast.

Advances in the state of the art of computer-controlled medical linear accelerators have recently become available that, along with newly developed treatment planning techniques, may provide significant improvements in the delivery and control of external beam radiation through beam-intensity modulation (Boesecke *et al* 1988, Brahme 1988, Convery and

Rosenbloom 1992, Leibel *et al* 1992, Webb 1992, 1997, LoSasso *et al* 1993, Powlis *et al* 1993, Chui *et al* 1994, Mageras *et al* 1994, Brewster *et al* 1995, Fraass *et al* 1995, Kutcher *et al* 1995, Mackie *et al* 1995, McShan *et al* 1995, Ling *et al* 1996, Boyer *et al* 1997). It is expected that using photon IMRT, the problem (a) above may be significantly improved but (b) may become more serious as treatment time increases with the number of fields/segments used (increased leakage or scattering dose). Using the modulated electron radiotherapy (MERT) technique (Lief *et al* 1996, Hyödynmaa *et al* 1996, Zackrisson and Karlsson 1996, Åsell *et al* 1997, Ebort and Hoban 1997, Karlsson *et al* 1998, 1999), on the other hand, problem (a) may also be significantly improved and problem (b) may almost be eliminated due to the nature of the electron beams.

In the optimization process of MERT, dose conformity along the beam direction can be achieved by modulating the electron incident energy, making use of the sharp dose fall-off feature. A drawback is its large penumbra at large depths. Traditionally, electron beams are shaped using a cutout (or blocks) and beam penetration/intensity may be modified using a bolus. However, it is time-consuming to make such beam modifiers and the treatment time would be significantly increased if such beam modifiers are used for MERT. Efforts have been made to use computer-controlled MLC for electron beam modulation. The recent results by Karlsson *et al* (1999) showed that by replacing the air in the treatment head with a low-cost, custom-made helium balloon, the beam penumbral width (20/80) was reduced from 18 to 11 mm at 80 cm SSD. The beam characteristics are affected by the position of the MLC. However, by replacing the air between the MLC and the patient with a helium balloon, the beam penumbra become almost the same as that achieved by electron beam-shaping with an electron applicator that extends to the patient skin surface (Karlsson *et al* 1999). This means that many of the techniques so far developed with computer-controlled MLC and our experience with MLC photon beam modulation can be adopted for use with MERT.

The calculation of dose distributions for electron beam radiotherapy planning is challenging because electron scattering is strongly affected by changes in density and composition in the patients. The 3D pencil beam algorithm (Hogstrom *et al* 1981) is a fast analytical algorithm which has been adopted by most treatment planning systems. However, it has limitations with small irregular electron fields and in the presence of inhomogeneities (Cygler *et al* 1987, Bielajew *et al* 1987, Mah *et al* 1989, Mackie *et al* 1994, Ma *et al* 1999). The Monte Carlo simulation has been demonstrated to be a viable option for such complex situations, and also the only way to take into account back-scattering from denser materials in a patient (e.g. bone or metal inserts) (Shortt *et al* 1986, Cygler *et al* 1987, Mackie *et al* 1994, Kawrokaw *et al* 1996, Mohan 1997, Kapur 1999, Ma *et al* 1999). The EGS4/BEAM system was developed for the simulation of radiotherapy beams from various radiotherapy treatment units, such medical accelerators (Rogers *et al* 1995). Excellent agreement (1–3%) has been achieved between the Monte Carlo dose distributions calculated using the simulated particle phase-space data and measurements (Rogers *et al* 1995, Kapur *et al* 1998, Zhang *et al* 1999, Ma *et al* 1999). We have installed a Monte Carlo patient dose calculation tool on a clinical treatment planning system (Ma *et al* 1999) and used Monte Carlo for treatment planning and dose delivery validation. This has reduced the uncertainty of the accelerator output for small irregular field electron beams from up to 10% to about 3% (Ma *et al* 1997, Kapur *et al* 1998).

Conformal radiotherapy was initially used to limit the normal tissue dose by conforming the treatment field to the beam's-eye-view projection of the target volume (Takahashi 1965). For photon beams, the MLC was used to collimate the fields and later to modulate the beam intensity in the field (Boesecke *et al* 1988, Brahme 1988, Convery and Rosenbloom 1992, Leibel *et al* 1992, Webb 1992, 1997, LoSasso *et al* 1993, Powlis *et al* 1993, Chui *et al* 1994, Mageras *et al* 1994, Brewster *et al* 1995, Kutcher *et al* 1995, Mackie *et al* 1995,
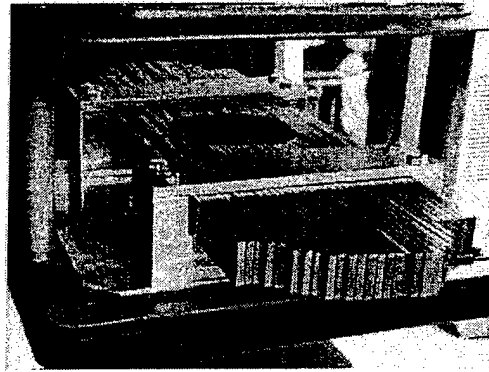
Figure 1. A prototype of an electron MLC mounted on the bottom scraper of a 25 cm × 25 cm applicator on a Varian Clinac 2100C accelerator. The MLC has 30 pairs of steel leaves and the leaf positions are fixed by the tightening screws.

McShan *et al* 1995, Ling *et al* 1996, Boyer *et al* 1997). There have been a few studies on electron conformal therapy. Tailoring dose distributions using electron beams requires substantial beam manipulation, due to their scattering characteristics. Such manipulation is already possible with radiation sources such as microtrons where preferential energy selection and magnetically scanned pencil beams are possible (Lief *et al* 1996). Both intensity- and energy/intensity-modulated electron beams have been investigated to conform the dose to the target near the surface (Lief *et al* 1996, Hyödynmaa *et al* 1996, Zackrisson and Karlsson 1996, Ebert and Hoban 1997, Karlsson *et al* 1998). More recent work has studied the combination of photon IMRT and MERT for targets at greater depth (Karlsson *et al* 1999). Using the helium-balloon technique together with a computer-controlled MLC, it may be possible to deliver a set of intensity-modulated beams with different energies and incident angles.

In this work, we investigate the feasibility of optimizing energy- and intensity-modulated electron beams for radiotherapy treatment. We report here our Monte Carlo studies of a multileaf collimator specially designed for MERT and some preliminary experimental results. We also report on the dose calculation algorithms and their effects on treatment plan optimization for MERT. We will discuss the differences in the beam characteristics between a photon MLC and an electron MLC. We will compare the dose distributions between a conventional tangential photon treatment plan and a MERT treatment plan for a hypothetical breast treatment to demonstrate the potential of MERT for target dose coverage and normal tissue sparing.

2. Materials and method

2.1. The prototype electron MLC

We have developed a prototype manual-driven electron MLC for the beam delivery for MERT. As shown in figure 1, the electron MLC consists of 30 steel leaf pairs, which were made from the off-the-shelf steel bars for convenience and cost-effectiveness. Each leaf is 0.476 cm wide, 20 cm long and 2.54 cm thick with straight edges and ends. The leaves were mounted on a steel frame, which can be attached to the bottom scraper of a 25 cm × 25 cm electron applicator on a Varian Clinac 2100C (Varian Oncology Systems, Palo Alto, CA). The leaves can slide in

the steel frame and the leaf positions can be easily set using a pre-cut cardboard for a beam segment. The field shape is maintained by tightening the screws from the side. The largest radiation field available using the electron MLC was 15.7 cm × 15.7 cm projected at 100 cm source–surface distance (SSD).

Because of the existing electronic device for inserting the electron cutout, the leaves could not be placed at the last scraper level without modifying the existing applicator geometry. Instead, the steel frame was inserted using the electron cutout mount and the leaves were placed immediately above the last scraper. This resulted in a slightly greater air gap (7 cm) between the bottom of the electron MLC leaves and the phantom surface (assuming a 97 cm SSD) compared with that of an electron cutout (5 cm for a 100 cm SSD). The projected leaf width for a 5 cm air gap is 0.5 cm, while for a 7 cm air gap the projected leaf width is 0.51 cm (e.g. for the current configuration at 97 cm SSD). Further modifications are needed to the electron applicator geometry in order to lower the electron MLC leaves. The ideal location for the MLC leaves is the last scraper since electron cutouts will no longer be needed if an electron MLC is in place.

Film measurement was performed to study the characteristics of the electron beams collimated by the electron MLC. The film was calibrated following the AAPM TG-25 recommendations (AAPM 1991) and the exposures were taken by placing film at different depths in a solid water phantom. The film was scanned using a film scanner which has a spatial resolution of about 0.15 cm.

2.2. The Monte Carlo beam simulation

We have used the EGS4 (Nelson *et al* 1985) user code BEAM for the accelerator head simulation. Detailed descriptions of the software can be found in Rogers *et al* (1995). A detailed description of the clinical implementation of the Monte Carlo method at the Stanford Medical Center was given in a previous publication (Ma *et al* 1999).

For this work, we have used the previously simulated Monte Carlo beam data for 6, 12 and 20 MeV electron beams from a Varian Clinac 2100C linear accelerator and for 6 MV photon beams from a 2300CD accelerator (Varian Oncology Systems, Palo Alto, CA). The dimensions and materials for the accelerator components were incorporated according to the manufacturer's specifications. Electron beams emerging from the vacuum exit window were assumed to be monoenergetic and monodirectional with a beam radius of 0.1–0.2 cm (Kapur *et al* 1998). The energy cutoffs for electron transport in the accelerator simulation (ECUT and AE) were 700 keV (kinetic + rest mass) and for photon transport (PCUT and AP) 10 keV. The electron transport step length was confined such that the maximum fractional energy loss per electron step is 4% (i.e. ESTEPE = 0.04). The ICRU recommended compositions and stopping power values were used for the materials in the accelerator simulations (ICRU 1984). The phase-space data were scored at a plane either immediately above the photon MLC or above the lowest scraper. The number of particles was about 2–30 million in an electron beam file and about 50 million in a photon file.

Field shaping by the photon MLC or electron MLC was further simulated using the BEAM component module MLC. MLC could simulate either straight or 'double focused' leaf edges and ends. In this work, we have simulated electron beams collimated by a photon MLC with both straight and double focused MLC leaf shapes. The leaves were 7.5 cm thick and made of tungsten. The leaf center was 49 cm from the isocentre. The intervening air in the accelerator and between the MLC and the isocentre was in some cases replaced with helium to investigate the effect of electron scattering in the air. In the simulations of the electron beams collimated by an electron MLC, the leaves were placed on the bottom scraper of a 25 cm × 25 cm applicator

with a 7 cm air gap between the bottom surface of the MLC and the isocentre. Tungsten leaves of 1.5 cm thickness with straight edges and ends were used in all the simulations and the phase space data were used in the subsequent dose calculations except for the leaf leakage study where different leaf materials and thicknesses were investigated for the electron MLC.

2.3. The Monte Carlo dose calculation

The EGS4 user code, MCDOSE (Ma *et al* 1999), was used in this work for the dose calculations. MCDOSE was designed for dose calculations in a 3D rectilinear voxel geometry. Voxel dimensions were completely variable in all three directions. Every voxel (volume element) could be assigned to a different material. The cross-section data for the materials used were available in a pre-processed PEGS4 cross-section data file. The mass density of the material in a MCDOSE calculation was varied based on the patient's CT data although the density effect corrections for the stopping powers of the material remain unchanged (Ma *et al* 1999). The voxel dimensions and materials were defined in a MCDOSE input file together with the transport parameters such as the energy cutoffs (ECUT and PCUT), the maximum fractional energy loss per electron step (ESTEPE), and the parameters required by PRESTA (Bielajew and Rogers 1987). Several variance reduction techniques have been implemented in the MCDOSE code to improve the calculation efficiency. These include photon interaction forcing, particle splitting, Russian roulette, electron range rejection and region rejection, particle track displacement and rotation, and correlated sampling. Detailed descriptions of these techniques have been given elsewhere (Rogers and Bielajew 1990, Ma and Nahum 1993, Rogers *et al* 1995, Kawrakow *et al* 1996, Keall and Hoban 1996, Ma *et al* 1999).

For patient dose calculations, the simulation phantom was built from the patient's CT data with up to $128 \times 128 \times 128$ voxels (uniform in any dimension). The side of a voxel varied from 0.2 to 0.4 cm. A separate program was developed to convert the patient's CT data from the FOCUS treatment planning system (Computerized Medical Systems, St Louis, MO) to desired dimensions, material types and densities. The organ contours were also obtained for dose calculation and analysis. The phase-space data obtained from a BEAM simulation were used as a source input with variable source positions and beam incident angles. To simulate the dose distribution of a finite size beamlet used by the inverse planning process, particles were transported to the MLC plane and only those within the beamlet area ($= 1$ cm $\times 1$ cm projected at 100 cm SSD) were allowed to go through. This ignored the bremsstrahlung photon leakage and electron scattering by the leaf ends in the optimization process (the effect was corrected in the final dose calculation, as discussed below). After optimization, a leaf sequence was generated using a modified 'step and shoot' algorithm based on our early work (Ma *et al* 1998). The final MERT dose distribution was computed based on an intensity map (a 2D distribution of particle weighting factors) reconstructed from the leaf sequence. The bremsstrahlung leaf leakage effect was included in the intensity map using the leaf sequence and pre-calculated leaf leakage data for 1.5 cm thick tungsten leaves. MCDOSE produced data files that contained geometry specifications such as the number of voxels in all the three directions and their boundaries as well as the dose values and the associated (1σ) statistical uncertainties in the individual voxels and organs (structures). The EGS4 transport parameters were ECUT = AE = 700 keV, PCUT = AP = 10 keV and ESTEPE = 0.04. The number of particle histories simulated ranged from 2 million to 30 million for a MERT treatment. The 1σ statistical uncertainty in the dose was generally 2% or smaller of the D_{max} value. The CPU time required for a MERT simulation was about 1–3 h on a Pentium III 450 MHz PC with the variance reduction option switched on.
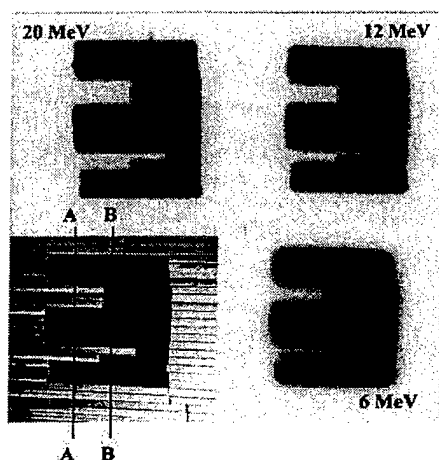
Figure 2. Beam intensity distributions measured by film on the surface of a solid water phantom for 6, 12 and 20 MeV electrons. The MLC leaf positions for the electron fields are also shown (bottom left).

2.4. The optimization process

The treatment planning optimization system used in this work is a home-developed system based on the work by Jiang (1998). First, the planner inputs the patient geometry and defines the treatment setup, such as the beam energy, number and orientations of beams, etc. The target volume and the critical structures are defined by the clinician. A reference monitor unit is assigned to each open rectangular beam and the dose deposition coefficients, which are defined as the dose contribution from a beamlet to a point, are calculated using the MCDOSE code.

Second, using the calculated dose deposition coefficients as input, the optimal intensity profile for each beam is achieved using a gradient method to minimize the objective function. For the target area, a quadratic form of objective function is specified. In addition, two target dose-uniformity constraints are used to ensure a uniform target dose distribution and to distinguish the clinical importance of cold and hot spots. For the critical structures, maximum-dose constraint and several levels of dose-volume constraints are assigned to each structure. For each objective function and constraint, an importance weight relative to the target objective function is assigned. All the constraints are mathematically transformed to the penalty functions of quadratic forms. The augmented objective function, which should be minimized, is a combination of the original objective functions and all penalty functions. The results of the optimization process are the intensity profiles for the individual fields (different incident energies and gantry angles). The same optimizer has been used for photon beam optimization with the Monte Carlo method and a finite-size pencil beam algorithm (Jiang 1998, Jiang *et al* 1999, Pawlicki *et al* 1999).

3. Results and discussion

3.1. Characteristics of electron beams collimated by an electron MLC

Figure 2 shows the electron fields collimated by the prototype electron MLC for 6, 12 and 20 MeV electron beams on a Varian Clinac 2100C machine. For convenience, a photo showing
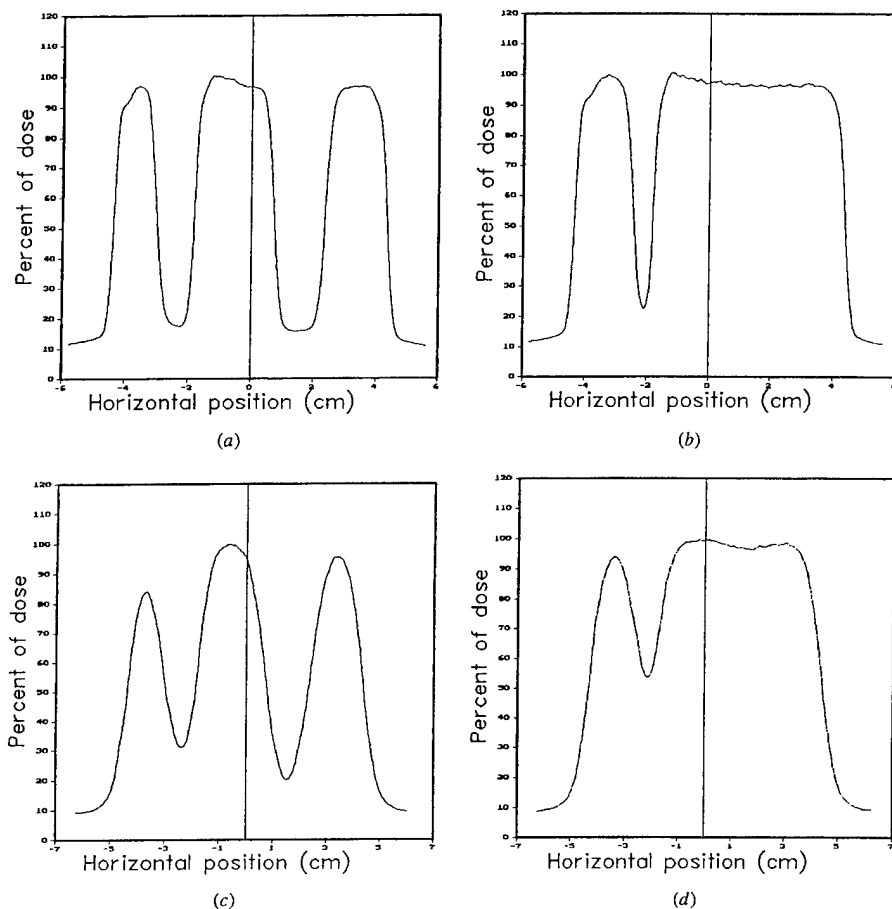
Figure 3. Beam profiles measured by film on the surface of a solid water phantom for the 6 MeV and 20 MeV electron fields shown in figure 2: (a) 20 MeV along A–A; (b) 20 MeV along B–B; (c) 6 MeV along A–A; (d) 6 MeV along B–B.

the MLC leaf positions for the field shape is also included in figure 2. Figure 2 shows the film measurement at the surface of a solid water phantom (97 cm SSD) for 6, 12 and 20 MeV electron beams. Figure 3 shows the measured profiles on the phantom surface along A–A and B–B for the 6 MeV and 20 MeV electron fields shown in figure 2. Figure 4 shows the beam profiles at 2 cm depth in the solid water phantom. It can be seen that for a 20 MeV electron beam, 0.5 cm leaf shapes are still distinguishable on the surface but become very blurred at 2 cm depth. For a 6 MeV electron beam, however, the effect of electron scattering becomes so severe that a leaf width smaller than 1.0 cm will not result in any improvement in the spatial resolution. However, a small leaf width may have the advantage of defining the field more precisely in the direction perpendicular to the leaves.

Based on these experimental results, we further performed Monte Carlo simulations of electron fields collimated by 1 cm wide leaves to study the effect of material type and
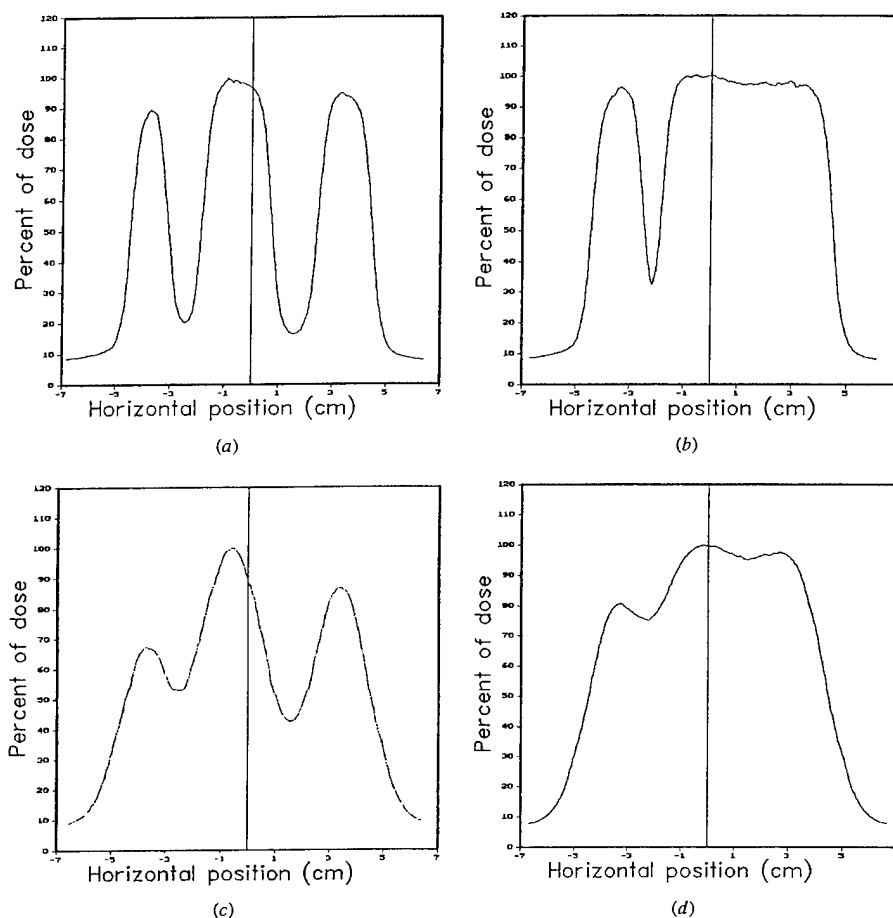
Figure 4. Beam profiles measured at 2 cm depth in a solid water phantom for the 6 MeV and 20 MeV electron fields shown in figure 2: (a) 20 MeV along A–A; (b) 20 MeV along B–B; (c) 6 MeV along A–A; and (d) 6 MeV along B–B.

leaf thickness. Although the beam penumbral widths did not change significantly for leaf thicknesses smaller than 2 cm, the beam intensity outside the field was affected by the leaf thickness and the atomic number of the leaf material. As shown in figure 5 for a 20 MeV electron beam, 1.5 cm thick zinc reduced the electron fluence outside the field to about 5% of the central axis value (figure 5(a)). These electrons were mainly generated by the bremsstrahlung photons in the MLC leaves. This was confirmed by the photon fluence as shown in figure 5(b), where 1.5 cm zinc MLC leaves resulted in about 60% higher photon fluence outside the field compared with the central axis photon fluence. Some electrons were also scattered off the leaf ends and by air. For 1.5 cm copper, 1.5 cm lead and 2 cm steel, the electron fluence was about 2.5% of the central axis value. The electron fluence was reduced to about 1.5% if the leaves were made of 1.5 cm tungsten. This was reflected by the 30% smaller photon fluence under the tungsten MLC leaves compared with the central axis photon fluence. Clearly, tungsten was superior to

Clinac 2100C 20 MeV 10cm x 10cm field

(a)

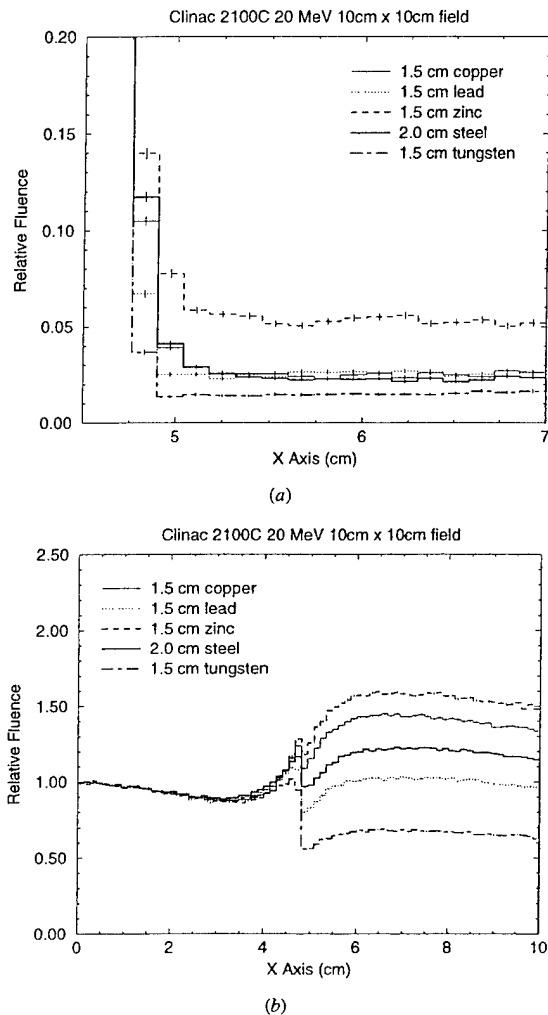Clinac 2100C 20 MeV 10cm x 10cm field

(b)

Figure 5. Monte Carlo simulated electron (a) and photon (b) planar fluence in the penumbral region and outside the treatment field for a Varian Clinac 2100C 20 MeV electron beam collimated by an electron MLC of different leaf materials and thicknesses. The air gap between the electron MLC and the scoring plane is 7 cm.

other materials in terms of leaf leakage. If we increased the tungsten leaf thickness to 2 cm the electron fluence would be reduced to less than 1% of the central axis value and the photon leakage would be reduced to about 50% of the central axis value (not shown).

To study the overall effect of the leaf leakage, leaf scattering, air scattering and the extended source in an electron beam, we compared the dose distributions for single fields and multiple abutting fields collimated by an electron MLC with 1.5 cm thick tungsten leaves. Figure 6 shows the Monte Carlo calculated dose distributions for a single 4 cm × 4 cm electron field and a multiple abutting field of the same size formed by four 1 cm × 4 cm electron fields. For
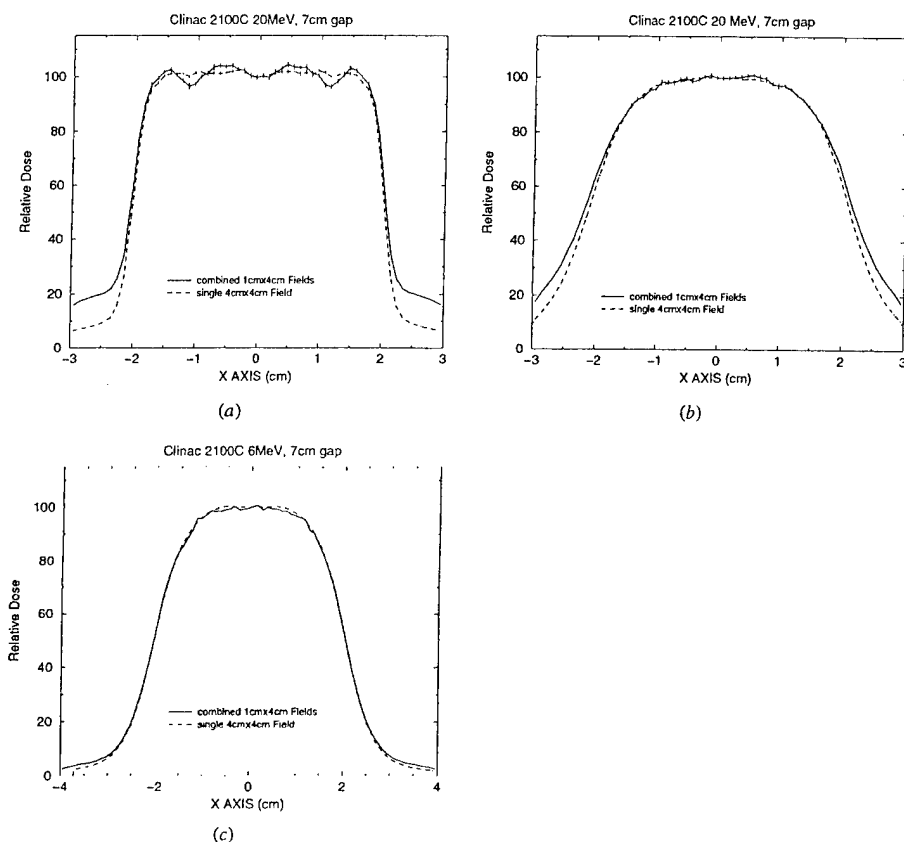
Figure 6. Monte Carlo calculated dose distributions in a water phantom for Varian Clinac 6 and 20 MeV electron beams collimated by an electron MLC of 1.5 cm thick tungsten leaves for a single 4 cm × 4 cm electron field and a 4 cm × 4 cm field formed by four 1 cm × 4 cm electron fields: (*a*) dose at surface for a 20 MeV beam; (*b*) dose at 3 cm depth for a 20 MeV beam; (*c*) dose at surface for a 6 MeV beam.

a 20 MeV electron beam, the dose at the phantom surface for the abutting field shows about 4% fluctuation compared with a single electron field (figure 6(*a*)). This is potentially due to the effect of leaf shape and extended source. The dose outside the field for the abutting field is about three times higher than that for the single field, which is mainly caused by the leaf leakage due to the longer beam-on time to deliver the four 1 cm × 4 cm fields and electron scattering off the leaf ends. The dose at 3 cm depth shows little difference between the abutting field and the single field except for the dose near the field edges and outside the field (figure 6(*b*)). For a 6 MeV electron beam, the dose at the phantom surface for the abutting field is almost the same as that for the single field (figure 6(*c*)). The dose outside the field for the abutting field is only slightly higher than that for the single field. The effect of leaf leakage is very small for a 6 MeV beam and the dose immediately outside the field is thought to be mainly due to the effect of electron scattering in the air. It seems that field abutting with 1 cm beamlets collimated by an electron MLC can provide adequate beam characteristics for MERT for the beam energies

investigated. However, the dose outside the field needs to be minimized through beam energy and leaf sequence optimization.

3.2. Comparisons of a photon MLC and an electron MLC

There have been studies on electron beam collimation using a photon MLC (Karlsson *et al* 1999). One of the advantages of using a photon MLC is the possibility of combining both photon and electron beams in the same plan. An essential requirement for matching a photon beam and an electron beam at different depths is that both beams share the same source position. Karlsson *et al* (1999) proposed several modifications to the design of a Varian Clinac 2300CD accelerator, one of which was to replace the intervening air with helium. This could significantly reduce the effect of electron scattering in the air on the beam penumbra. However, filling the accelerator head with helium requires major modifications to the existing accelerator design. In this work, we have investigated an alternative solution—a thin leaf MLC at the electron cutout level to reduce the air scattering effect. As can be seen in figure 7, the unfocused MLC leaf ends could scatter the electrons very significantly to degrade the beam characteristics near the field edges. The Varian MLC has rounded leaf ends, which are expected to have similar dosimetric characteristics as the unfocused MLC studied here. Focused leaf ends could greatly improve the beam edges and provided even slightly better dose profiles inside the field for a 20 MeV electron beam compared with an electron MLC (figures 7(a)–(c)), primarily due to the reduction of electron scattering in the accelerator head (helium versus air). The dose outside the field was slightly lower for the electron MLC than for the photon MLC. For a 6 MeV beam, an electron MLC gave slightly better surface dose profiles both inside and outside the field than the focused and unfocused photon MLC. However, the dose profiles became practically similar at the depth of the maximum dose and greater depths (not shown). Note that in these comparisons, we have placed the phantom surface at 20 cm below the photon MLC and 7 cm below the electron MLC to minimize the effect of electron scattering in the air or helium between the MLC and the phantom. It is evident that an electron MLC will have similar dosimetric characteristics as a photon MLC with focused leaf ends but without the need to replace the air in the accelerator head with helium.

3.3. Comparison of beamlet distributions

The accuracy of the beamlet distribution calculation may play an important role in the treatment planning optimization process. Ma *et al* (1999) reported significant differences in the final dose distributions of the optimized treatment plans computed by a commercial inverse treatment planning system with a finite-size pencil beam and the Monte Carlo method. Pawlicki *et al* (1999) demonstrated that inaccurate beamlet distributions may result in under-dosing in the target and over-dosing in the adjacent critical structures, and using the Monte Carlo calculated beamlets could potentially reduce the uncertainty in the photon IMRT dose distributions. This was demonstrated again by Jeraj and Keall (1999) using a Monte Carlo dose calculation based inverse planning algorithm.

It has been shown that the electron beam dose distributions calculated by the pencil beam algorithm as implemented in some commercial treatment planning systems could be fairly uncertain in the regions near material interfaces and inhomogeneities (Cygler *et al* 1987, Shortt *et al* 1986, Mackie *et al* 1994, Ma *et al* 1999). We have computed the beamlet dose distributions using the 3D pencil beam as implemented in the FOCUS treatment planning system (Computerized Medical Systems, St Louis, MO) and compared them with the Monte Carlo calculated beamlets. Figure 8 shows the dose distributions calculated using the Monte
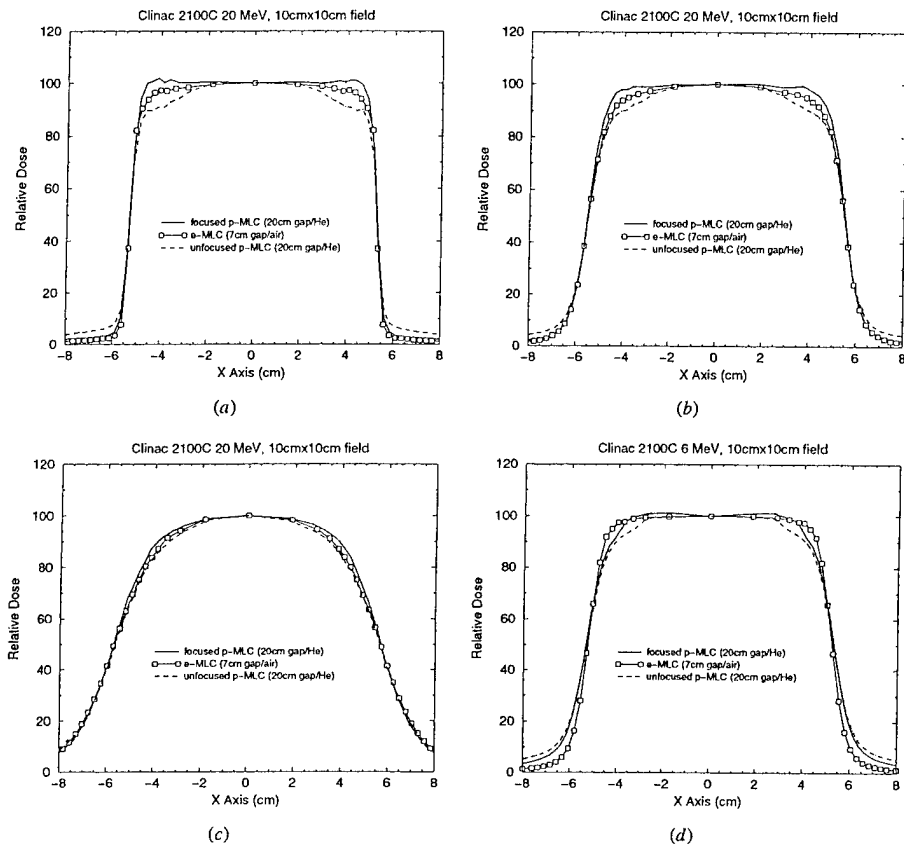
Figure 7. Monte Carlo calculated dose distributions in a water phantom for a 10 cm × 10 cm field collimated by an electron MLC with 1.5 cm thick tungsten leaves and a photon MLC with 7.5 cm thick leaves on a Varian Clinac 2100C accelerator: (a) surface dose for a 20 MeV beam; (b) dose at 3 cm depth for a 20 MeV beam; (c) dose at 6 cm depth for a 20 MeV beam; (d) surface dose for a 6 MeV beam. The electron MLC has straight leaf ends. The photon MLC has either straight or double-focused leaves.

Carlo method (a, c, e) and the FOCUS 3D pencil beam algorithm (b, d, f) for a 1 cm × 1 cm 12 MeV beamlet incident on a patient phantom built from CT data. For beamlets with normal incidence (figures 8(a) and (b)), the difference in the dose distributions in the heart was evident: the Monte Carlo calculated isodose lines varied with the heart contour while the pencil beam isodose lines remained symmetrical despite the change in material densities. Figures 8(c) and (d) show the beamlet distributions with a 10 cm air gap. The difference is clearly seen near the surface. The beamlet distributions again differed significantly in the lung for oblique incidence (figures 8(e) and (f)). The axis of the beamlet was intentionally placed to go through soft tissues and bones. The pencil beam isodose lines seemed to stretch according to the beam axis pathlength and showed no signs of electron build-down near the low-density material. These results provided enough evidence to show that to ensure the accuracy of the optimized dose distributions for MERT we should use the Monte Carlo method to compute the electron beamlets for the inverse planning process.

Figure 8. Dose distributions calculated using the Monte Carlo method (a, c, e) and the FOCUS 3D pencil beam algorithm (b, d, f) for a 1 cm $\times$ 1 cm 12 MeV beamlet with normal incidence (a and b), normal incidence plus 10 cm air gap (c and d), and oblique incidence (e and f). The beamlet size is defined at 100 cm SSD. The isodose lines shown are 10, 20, 30, 40, 50, 60, 70, 80 and 90% of the maximum dose respectively.

3.4. MERT versus photons: a hypothetical treatment plan

Modulated electron radiotherapy is a general purpose technique that should be advantageous in many clinical situations. An exhaustive investigation of the specific advantages of MERT
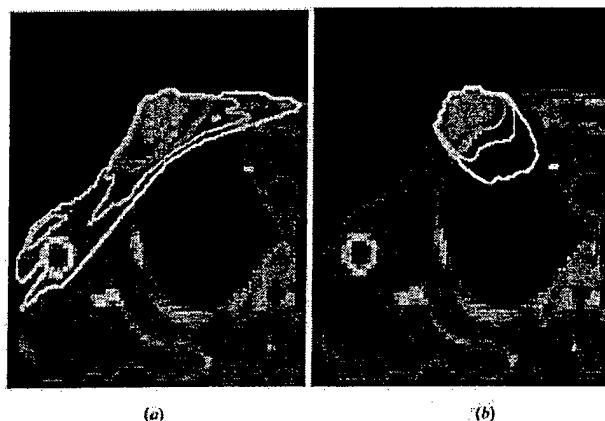
Figure . Treatment plans for a hypothetical breast case using tangential 6 MV photon beams (*a*) and MERT with 6, 12 and 20 MeV electron beams (*b*). Both plans were calculated using the Monte Carlo method. The isodose lines (90, 70, 50 and 30%) represented 50, 38.9, 25 and 16.7 Gy.

over traditional treatment modalities on a site by site basis is outside the scope of this work. However, to demonstrate the possibility of improving the dose homogeneity in the target and the reduction of the dose in surrounding normal tissues, we compare the dose distributions to treat a hypothetical target using tangential photon beams and MERT. The purpose of the comparison was to illustrate the concept of MERT but not to draw specific conclusions on the use of either technique. Previous investigators have used artificial phantoms and hypothetical targets to mimic different treatment sites (e.g. Hyödynmaa *et al* 1996, Åsell *et al* 1997, Ebert and Hoban 1997). We considered it to be clinically relevant to use a more realistic patient geometry (built from CT data) in our comparison, although the target definition and beam setup are somewhat arbitrary. Figure 9 shows the hypothetical treatment plan using tangential 6 MV photon beams and MERT with normally incident 6, 12 and 20 MeV electron beams. The intensity maps for each electron beam energy are shown in figure 10. The beamlet size was 1 cm × 1 cm at 100 cm at isocentre. It is worth noting here, that as a matter of practicality, it is impossible to create the intensity maps shown in figure 10 using the conventional electron cutout approach but the electron MLC is a viable alternative. The dose distributions for both plans were calculated using the Monte Carlo method. The isodose lines (90, 70, 50 and 30%) were normalized in such a way that the 90% isodose surface would receive the prescribed target dose of 50 Gy. For the photon plan, the 90% dose line also included a margin in the lung to account for the effect of patient breathing. This was not needed for the electron plan as the electron beams were incident *en face* and the electron beamlet dose distributions do not vary significantly with breathing. Figure 11 shows the dose volume histograms (DVH) for the hypothetical treatment plans shown in figure 9. The target DVH together with the right lung DVH are shown in figure 11(*a*) (as percentage volume) and the right lung DHV and the 'total body' (including everything inside the external contour) DVH are shown in figure 11(*b*) (as absolute volume).

It is clear that MERT provided better dose homogeneity in the target region than tangential photon beams. Tangential photon beams produced hot spots in the target and cold spots near the skin (figure 11(*a*)). MERT significantly reduced the dose to the lung relative to tangential photon beams; the maximum dose to the lung was reduced from 50 Gy for a tangential treatment to 35 Gy for MERT (figure 11(*a*)). However, MERT increased the volume of the lung that
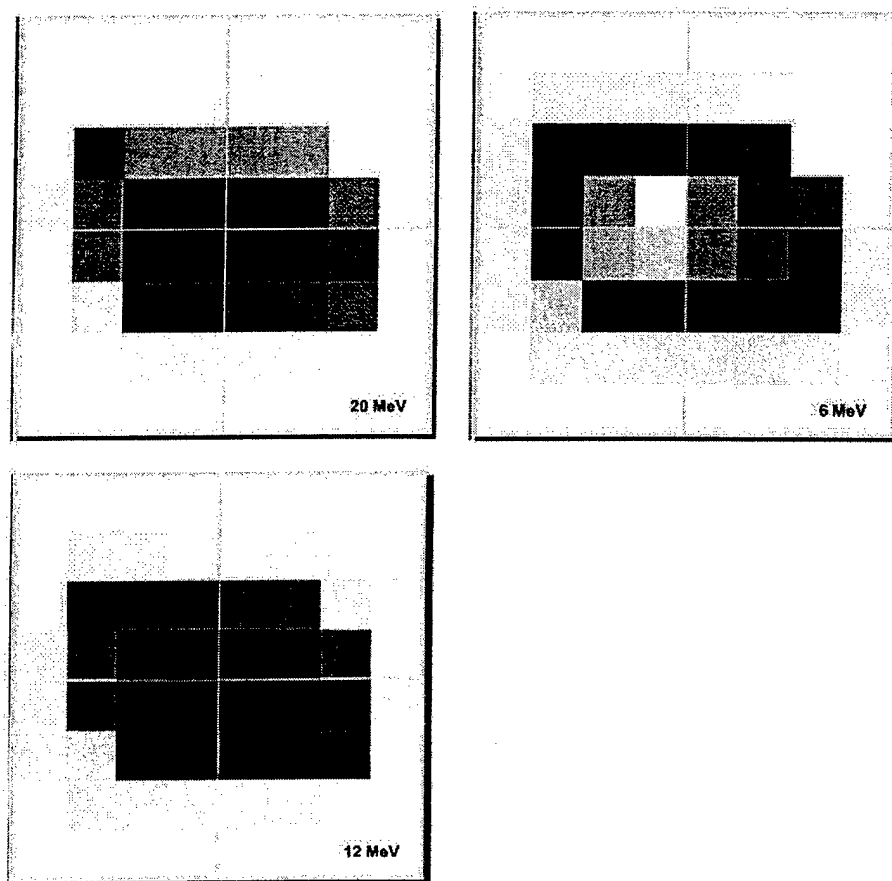
Figure 10. Intensity maps for the three electron beam energies. The beamlet size for each port was 1×1 cm^2. Darker beamlets indicate a higher weight than the lighter beamlets and the grey scale for all three maps is in absolute terms.

received a lower dose (10% more volume received 5 Gy and 20% more volume received 2 Gy) compared with tangential photon beams. The clinical significance of the increased lung volume receiving such a low dose needs to be investigated. On the other hand, over 150 cm^3 of lung received much less dose with MERT compared with tangential photon beams, which could result in reduced lung complications (figure 11(*b*)). Another clear benefit with MERT is the exclusion of the surrounding normal tissue from the high dose volume (figure 11(*b*)). Over 1000 cm^3 of normal tissue received 10–30 Gy less dose in a MERT plan compared with this tangential photon beam plan.

4. Conclusions

In this work, we have investigated the feasibility of modulating both energy and intensity of electron beams for radiotherapy. This was achieved by combining electron beams of different
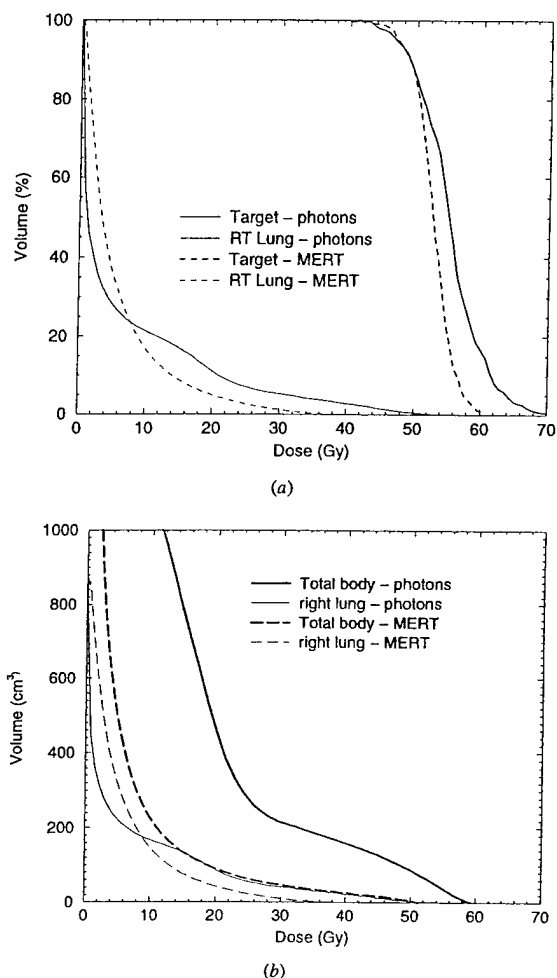
Figure 11. Dose volume histograms (DVH) for the breast treatment plans shown in figure 9: (a) DVH shown as percentage volume for the target (PTV) and the right lung and (b) DVH shown as absolute volume for the right lung and the 'total body' which includes everything inside the external contour.

nominal energies and variable intensity distributions. A prototype electron MLC was built to study the characteristics of MLC-collimated electron beams and the Monte Carlo simulations were used to investigate the effect of MLC leaf material, thickness, shape and location. The beamlet distributions calculated using a 3D electron pencil beam algorithm as implemented in a commercial treatment planning system and the Monte Carlo method were compared for electron beams of different energies, extended air gaps, oblique incidence and heterogeneous geometries. A hypothetical breast case was used to compare the dose distributions using tangential photons and MERT for target coverage (dose homogeneity) and normal tissue sparing (dose reduction in the lung and other surrounding normal tissues).

Our results showed that an electron MLC at the electron cutout location can provide adequate beam collimation for MERT without the need to replace the air in the accelerator head and between the MLC and the phantom with helium. The beam characteristics collimated by an electron MLC are comparable to those collimated by a focused photon MLC. However, the latter requires the accelerator head and between the MLC and the phantom to be filled with helium, which may be impractical for some accelerators because of the major modifications needed to the structure design. An electron MLC can also be used in place of a cutout. The Monte Carlo method can accurately simulate particle transport in cases involving extended air gaps, oblique incidence and heterogeneous anatomy, and is therefore suitable for the beamlet calculation for MERT treatment optimization. Our preliminary results based on a hypothetical breast case demonstrated the potential of MERT for uniform target coverage and normal tissue sparing. To fully explore the potential of MERT, further studies need to be carried out for realistic clinical cases and for other treatment sites such as the head and neck.

Ac no ledgments

References

AAPM 1983 AAPM TG-21, a protocol for the determination of absorbed dose from high-energy photons and electrons *Med. Phys.* 10 741
——1991 AAPM TG-25, Clinical electron beam dosimetry: report of AAPM Radiation Therapy Committee Task Group No. 25 *Med. Phys.* 18 73–109
Åsell M, Hyödynmaa S, Gustafsson A and Brahme A 1997 Optimization of 3D conformal electron beam therapy in inhomogeneous media by concomitant fluence and energy modulation *Phys. Med. Biol.* 42 2083–100
Bielajew A and Rogers D W O 1987 PRESTA—the parameter reduced electron step algorithm for electron Monte Carlo transport *Nucl. Instrum. Methods* B 18 165–81
Bielajew A F, Rogers D W O, Cygler J and Battista J J 1987 A comparison of electron pencil beam and Monte Carlo calculational methods *The Use of Computers in Radiation Therapy* ed I A D Bruinvis (Amsterdam: Elsevier) pp 65–8
Boesecke R, Doll J, Bauer B, Schlegel W, Pastyr O and Lorenz M 1988 Treatment planning for conformation therapy using a multileaf collimator *Strahlenther. Onkol.* 164 151–4
Brewster L, Mohan R, Mageras G, Burman C, Leibel S and Fuks Z 1995 Three dimensional conformal treatment planning with multileaf collimators *Int. J. Radiat. Oncol. Biol. Phys.* 33 1081–9
Boyer A L, Geis P B, Grant W, Kendall R and Carol M 1997 Modulated-beam conformal therapy for head and neck tumors *Int. J. Radiat. Oncol. Biol. Phys.* 3 227–36
Brahme A 1988 Optimal setting of multileaf collimators in stationary beam radiation therapy *Strahlenther. Onkol.* 164 343–50
Chui C S, LoSasso T and Spirou S 1994 Dose calculations for photon beams with intensity modulation generated by dynamic jaw or multileaf collimators *Med. Phys.* 21 1237–43
Convery D J and Rosenbloom M E 1992 The generation of intensity-modulated fields for conformal radiotherapy by dynamic collimation *Phys. Med. Biol.* 37 1359–74
Cygler J, Battista J J, Scrimger J W, Mah E and Antolak J 1987 Electron dose distributions in experimental phantoms: a comparison with 2D pencil beam calculations *Phys. Med. Biol.* 32 1073–83
DeMarco J J, Solberg T D and Smathers J B 1998 A CT-based Monte Carlo simulation tool for dosimetry planning and analysis *Med. Phys.* 25 1–11

Ebert M A and Hoban P W 1997 Possibilities for tailing dose distributions through the manipulation of electron beam characteristics *Phys. Med. Biol.* **42** 2065–81

Faddegon B A, Balogh J, Mackenzie R and Scora D 1998 Clinical considerations of Monte Carlo for electron radiotherapy treatment planning *Radiat. Phys. Chem.* **53** 217–28

Fraass B A, McShan D L, Kessler M L, Matrone G M, Lewis J D and Weaver T A 1995 A computer-controlled conformal radiotherapy system I: overview *Int. J. Radiat. Oncol. Biol. Phys.* **33** 1139–57

Hogstrom K R, Mills M D and Almond P R 1981 Electron beam dose calculations *Phys. Med. Biol.* **26** 445–59

Hyödynmaa S, Gastafsson A and Brahme A 1996 Optimization of conformal electron beam therapy using energy- and fluence-modulated beams *Med. Phys.* **23** 659–66

ICRU 1984 Radiation dosimetry: Stopping powers for electrons and positrons *ICRU Report* 37 (Bethesda, MD: ICRU)

Jeraj R and Keall P 1999 Monte Carlo-based inverse treatment planning *Phys. Med. Biol.* **44** 1885–96

Jiang S B 1998 Development of a compensator based intensity modulated radiation therapy system *PhD Thesis* Medical College of Ohio, Toledo, OH

Jiang S B, Boyer A L and Ma C-M 1999 A hybrid system for IMRT inverse planning and dose verification *Int. J. Radiat. Oncol. Biol. Phys.* **41** 123

Kapur A 1999 Monte Carlo dose calculations for clinical electron and intensity modulated photon beams in radiotherapy *PhD Thesis* Stanford University, Stanford, CA, USA

Kapur A, Ma C-M, Mok E and Findley D 1997 Characterization of small field electron beams for radiotherapy using Monte Carlo simulations *Proc. 12th Int. Conf. on the Use of Computers in Radiation Therapy (Salt Lake City, Utah)* (Madison, WI: Medical Physics Publishing) pp 157–8

Kapur A, Ma C-M, Mok E, Findley D and Boyer A L 1998 Monte Carlo calculations of clinical electron beam output factors *Phys. Med. Biol.* **43** 3479–94

Karlsson M G, Karlsson M K and Ma C-M 1999 Treatment head design for multileaf collimated high-energy electrons *Med. Phys.* **26** 2125–32

Karlsson M K, Karlsson M G and Zackrisson B 1998 Intensity modulation with electrons: calculations, measurements and clinical applications *Phys. Med. Biol.* **43** 1159–69

Kawrakow I, Fippel M and Friedrich K 1996 3D electron dose calculation using a voxel based Monte Carlo algorithm *Med. Phys.* **23** 445–57

Keall P J and Hoban P 1996 Superposition dose calculation incorporating Monte Carlo generated electron track kernels *Med. Phys.* **23** 479–85

Kutcher G J, Mageras G S and Leibel S A 1995 Control, correction and modeling of setup errors and organ motion *Semin. Radiat. Oncol.* **5** 134–45

Leibel S A *et al* 1992 Three-dimensional conformal radiation therapy at the Memorial Sloan-Kettering Cancer Center *Semin. Radiat. Oncol.* **2** 274–89

Lief E P, Larsson A and Humm J L 1996 Electron dose profile shaping by modulation of a scanning elementary beam *Med. Phys.* **23** 33–44

Ling C C *et al* 1996 Conformal radiation treatment of prostate cancer using inversely-planned intensity-modulated photon beams produced with dynamic multileaf collimation *Int. J. Radiat. Oncol. Biol. Phys.* **35** 731–40

LoSasso T, Chui C S, Kutcher G J, Leibel S A, Fuks Z and Ling C C 1993 The use of multileaf collimators for conformal radiotherapy of carcinomas of the prostate and nasopharynx *Int. J. Radiat. Oncol. Biol. Phys.* **25** 161–70

Ma C-M, Mok E, Kapur A and Findley D 1997 Improvement of small-field electron beam dosimetry by Monte Carlo simulations *Proc. 12th Int. Conf. on the Use of Computers in Radiation Therapy (Salt Lake City, Utah)* (Madison, WI: Medical Physics Publishing) pp 159–62

Ma C-M, Mok E, Kapur A, Pawlicki T A, Findley D, Brain S, Forster K and Boyer A L 1999 Clinical implementation of a Monte Carlo treatment planning system for radiotherapy *Med. Phys.* **26** 2133–43

Ma C-M and Nahum A E 1993 Calculation of absorbed dose ratios using correlated Monte Carlo sampling *Med. Phys.* **20** 1189–99

Ma C-M, Reckwerd P, Holmes M, Rogers D W O and Geiser B 1995 DOSXYZ Users Manual *National Research Council Report* PIRS-0509(B) (Ottawa: NRC)

Ma L, Boyer A L, Xing L and Ma C-M 1998 An optimized leaf setting algorithm for beam intensity modulation using dynamic multileaf collimators *Phys. Med. Biol.* **43** 1629–43

Mackie T R, Holmes T W, Reckwerdt P J and Yang J 1995 Tomotherapy: optimized planning and delivery of radiation therapy *Int. J. Imaging Syst. Technol.* **6** 43–55

Mackie T R *et al* 1994 The OMEGA project: comparison among EGS4 electron beam simulations, 3D Fermi–Eyges calculations, and dose measurements *Proc. 11th Int. Conf. on the Use of Computers in Radiation Therapy (Manchester, UK)* pp 152–3

Mageras G S *et al* 1994 Initial clinical experience with computer-controlled conformal radiotherapy using the MM50 microtron *Int. J. Radiat. Oncol. Biol. Phys.* 30 971–8

Mah E, Antolak J, Scrimger J W and Pattista J J 1989 Experimental evaluation of a 2D and 3D pencil beam algorithm *Phys. Med. Biol.* 34 1179–94

McShan D L, Fraass B A, Kessler M L, Matrone G M, Lewis J D and Weaver T A 1995 A computer-controlled conformal radiotherapy system. II: sequence processor *Int. J. Radiat. Oncol. Biol. Phys.* 33 1159–72

Mohan R 1997 Why Monte Carlo? *Proc. 12th Int. Conf. on the Use of Computers in Radiation Therapy (Salt Lake City, UT)* (Madison, WI: Medical Physics Publishing) pp 16–18

Nelson R, Hirayama H and Rogers D W O 1985 The EGS4 code system *Stanford Linear Accelerator Center Report* SLAC-265 (Stanford, CA: SLAC)

Pawlicki T A, Jiang S B, Deng J, Li J S and Ma C-M 1999 Monte Carlo calculated beamlets for photon beam inverse planning *Med. Phys.* 26 1064–5

Powlis W D *et al* 1993 Initiation of multileaf collimator conformal radiation therapy *Int. J. Radiat. Oncol. Biol. Phys.* 25 171–9

Rogers D W O and Bielajew A F 1990 Monte Carlo techniques of electrons and photons for radiation dosimetry *Dosimetry of Ionizing Radiation* vol III, ed K Kase, B E Bjarngard and F H Attix (New York: Academic) pp 427–539

Rogers D W O, Faddegon B A, Ding G X, Ma C-M, Wei J S and Mackie T R 1995 BEAM: a Monte Carlo code to simulate radiotherapy treatment units *Med. Phys.* 22 503–25

Shortt K R, Ross C K, Bielajew A F and Rogers D W O 1986 Electron beam dose distributions near standard inhomogeneities *Phys. Med. Biol.* 31 235–49

Takahashi S 1965 Conformation radiotherapy-rotation techniques as applied to radiography and radiotherapy of cancer *Acta Radiol. Suppl.* 242 1–142

Wang L, Chui C and Lovelock M 1998 A patient-specific Monte Carlo dose-calculation method for photon beams *Med. Phys.* 25 867–78

Webb S 1992 Optimization by simulated annealing of three-dimensional conformal treatment planning for radiation fields defined by multi-leaf collimator: II. Inclusion of two-dimensional modulation of x-ray intensity *Phys. Med. Biol.* 37 1689–704

——1997 *The Physics of Conformal Radiotherapy: Advances in Technology* (Bristol: Institute of Physics Publishing)

Yu C X, Symons J M, Du M N, Martinez A A and Wong J W 1995 A method for implementing dynamic photon beam intensity modulation using independent jaws and multileaf collimators *Phys. Med. Biol.* 40 769–87

Zackrisson B and Karlsson M 1996 Matching of electron beams for conformal therapy of target volumes at moderate depths *Radiother. Oncol.* 3 261–70

Zhang G G, Rogers D W O, Cygler J E and Mackie T R 1999 Monte Carlo investigation of electron beam output factors versus size of square cutout *Med. Phys.* 26 743–50

Validation of a Monte Carlo dose calculation tool for radiotherapy treatment planning

J S Li, T Pawlicki, J Deng, S B Jiang, E Mok and C-M Ma

Department of Radiation Oncology, Stanford University School of Medicine, Stanford, CA 94305, USA

E-mail: jsli@reyes.stanford.edu

Abstract. A new EGS4/PRESTA Monte Carlo user code, MCDOSE, has been developed as a routine dose calculation tool for radiotherapy treatment planning. It is suitable for both conventional and intensity modulated radiation therapy. Two important features of MCDOSE are the inclusion of beam modifiers in the patient simulation and the implementation of several variance reduction techniques. Before this tool can be used reliably for clinical dose calculation, it must be properly validated. The validation for beam modifiers has been performed by comparing the dose distributions calculated by MCDOSE and the well-benchmarked EGS4 user codes BEAM and DOSXYZ. Various beam modifiers were simulated. Good agreement in the dose distributions was observed. The differences in electron cutout factors between the results of MCDOSE and measurements were within 2%. The accuracy of MCDOSE with various variance reduction techniques was tested by comparing the dose distributions in different inhomogeneous phantoms with those calculated by DOSXYZ without variance reduction. The agreement was within 1.0%. Our results demonstrate that MCDOSE is accurate and efficient for routine dose calculation in radiotherapy treatment planning, with or without beam modifiers.

(Some figures in this article are in colour only in the electronic version; see www.iop.org)

1. Introduction

With the rapid development of computer technology, the Monte Carlo technique, currently the most accurate method for dose calculation (Shortt *et al* 1986, Mackie 1990, Rogers and Bielajew 1990, Andreo 1991, Mackie *et al* 1994, DeMarco *et al* 1998, Ma *et al* 1999a), is becoming more practical for use in radiation therapy treatment planning systems. It has been argued that the outcome of radiation therapy treatment may be improved by using Monte Carlo dose calculation (Mohan 1997, Nahum 1997), especially for intensity modulated radiotherapy (IMRT) treatment planning (Jeraj and Keall 1999, Ma *et al* 1999a, 2000a, b). The Monte Carlo method is being developed for treatment planning dose calculations by several groups (Mackie 1990, Hartmann-Siantar *et al* 1997, Ma *et al* 1997, 1999a, DeMarco *et al* 1998, Wang *et al* 1998, Mubata *et al* 1998, Libby *et al* 1998, Faddegon *et al* 1998).

At present, there are several general-purpose Monte Carlo codes in widespread use for radiation transport simulation, e.g. Electron Gamma Shower version 4 (EGS4) (Nelson *et al* 1985), ETRAN/ITS (Berger and Seltzer 1987) and Monte Carlo *N*-particle (MCNP) (Hendricks 1994) and PENELOPE (Salvat *et al* 1996). It is well known that the EGS4 code system is very well documented and it has been thoroughly benchmarked in the energy region of dosimetric interest (Rogers 1984a, b, Rogers and Bielajew 1984, 1986, 1990). DOSXYZ is

an EGS4 based Monte Carlo simulation code for calculation dose distribution in a rectilinear voxel phantom (Rogers *et al* 1995, Ma *et al* 1995). It is also well benchmarked. Comparisons of the DOSXYZ results with measurements have been reported previously (Rogers *et al* 1995, Kapur *et al* 1998, Ma 1998, Zhang *et al* 1999, Ma *et al* 1999a, 2000a). Unfortunately, these codes are too slow to be acceptable for routine dose calculation in treatment planning systems with existing hardware. Some codes based on the Monte Carlo method have been developed to speed up the dose calculation, such as Macro Monte Carlo (MMC) (Neuenschwander and Born 1992, Neuenschwander *et al* 1995), Voxel Monte Carlo (VMC and XVMC) (Kawrakow *et al* 1996, Fippel 1999) and Super Monte Carlo (SMC) (Keall and Hoban 1996a). Further verification and improvements are needed for routine treatment planning dose calculations.

A new EGS4/PRESTA (Bielajew and Rogers 1987) user code, MCDOSE, has been developed for routine clinical dose calculation (Ma *et al* 1999b, 2000c). MCDOSE was designed as a dose calculation module for easy implementation in a radiotherapy treatment planning system. We have implemented it in an existing commercial RTP system for conventional photon/electron beams (Ma *et al* 1999a) and intensity modulated radiotherapy (IMRT) dose verification (Ma *et al* 2000a). MCDOSE shares similar structure and geometry definition with other EGS4 user codes, such as DOSXYZ. MCDOSE and DOSXYZ have some common features. They can both simulate the transport of photons and electrons (and positrons) in a 3D rectilinear phantom geometry. The volume elements (voxels) in the phantom can have uniform or variable dimensions and the material in the voxel can be specified by the user or determined from the electron density data derived from the patient CT data. Source models are supported in both codes. But there are other features in MCDOSE, which are absent in DOSXYZ:

(a) Advanced multiple-source models (Ma *et al* 1997, Ma 1998, Deng *et al* 2000, Jiang *et al* 2000a, b) are used as source input for both photon and electron beams in MCDOSE. The multiple-source models implemented in MCDOSE are more accurate and flexible, and easy for commissioning.

(b) Beam modifiers such as jaws, wedges, blocks, compensators, electron cutouts and bolus are included by MCDOSE in the patient simulation. Both static and dynamic MLC fields can be simulated for conventional and intensity modulated radiotherapy.

(c) Several variance-reduction techniques have been implemented in MCDOSE. Both codes have range rejection. However, it was implemented in different ways and in different simulation procedures.

(d) There is an option for selecting the geometry coordinates from two definitions in MCDOSE. One (x, y, z) is the same as that in DOSXYZ for phantom study. The other (x', y', z') is for convenient patient dose calculation corresponding to the treatment system. The relationship between the two coordinates is $x = x'$, $y = -z'$ and $z = y'$.

(e) Beamlets dose calculation for Monte Carlo inverse planning can be performed by MCDOSE for both photon and electron beams.

(f) MCDOSE can produce dose volume histograms (DVH) using the patient contour information.

The inclusion of beam modifiers and the implementation of variance reduction techniques makes MCDOSE more practical for routine dose calculation. Beam modifiers play an important role in radiotherapy treatment. They modify the beam shape and/or intensity distribution and therefore change the dose distribution in the patient. They need to be considered for treatment planning dose calculations. It is not sufficient to treat jaws and blocks as apertures and to change the profile using the wedge or compensator factors conventionally. The effect of beam modifiers has been studied by Schach von Wittenau *et al* (2000). It was found

that the scattered electrons generated in jaws could increase the surface dose by several per cent depending on the beam energy and field size. The photon transmission and bremsstrahlung generated in the modifiers need to be considered. To ensure simulation accuracy, these beam modifiers should be simulated with accurate geometry when the Monte Carlo method is used for routine dose calculation. Some codes, like BEAM and PEREGRINE (Walling *et al* 1998), can be used to simulate beam modifiers. But BEAM can only simulate them separately from patient dose calculation. One has to simulate particle transport in the beam modifiers using BEAM first. After scoring the phase space below the modifiers, dose calculation in the patient phantom can then be performed (Ma *et al* 1999a). This two-step method works well but is inconvenient and can be time-consuming. It is not suitable for routine dose calculations. The inclusion of beam modifiers into the patient dose calculation simplifies the simulation procedure in terms of simulation steps and intermediate data storage. Although Monte Carlo is an accurate method, the CPU time needed to perform statistically meaningful dose calculation is always a problem that prevents it from being applied in routine dose calculations. The variance reduction techniques implemented in MCDOSE generally speed up the dose calculation by a factor of 10–30 (Ma *et al* 2000c). This makes the code more practicable for routine application. The dose calculation using MCDOSE for a nine-field IMRT plan (including pre- and post-optimization dose calculation) can be finished in 1 to 4 h on a 450 MHz Pentium III personal computer (Pawlicki *et al* 1999, Ma *et al* 2000b).

Before MCDOSE can be used reliably for clinical dose calculation, it must be extensively validated. The accuracy of the dose calculation depends on the input beam data and the implementation of the user code. Source modelling and beam commissioning have been investigated by Ma *et al* (1997), Ma (1998), Deng *et al* (2000) and Jiang *et al* (2000a, b). Excellent agreement in dose distributions in both homogeneous and heterogeneous phantoms has been achieved between source model, phase space data and measurements. In this work, we focus on the validation of the user code for beam modifiers and variance reduction techniques. The geometry description for beam modifiers and the implementation of variance reduction techniques may affect the simulation accuracy of the code.

The validation of beam modifiers was performed by comparing the simulation results of MCDOSE with those of BEAM/DOSXYZ. The dose distributions in specifically designed homogeneous and inhomogeneous phantoms with different source inputs calculated using MCDOSE and DOSXYZ are presented. Machine data for two Varian accelerators, Clinac 2100C and 2300C/D, were measured as required by the commissioning procedure.

2. Materials and methods

2.1. Simulation of beam modifiers in MCDOSE

In this work, we have implemented beam modifier simulation in MCDOSE. The combination of the modifiers, the geometry parameters and materials can be input by the user. Several different modifiers can be used together. Each of them occupies a slab. For photon beams our multiple-source model covers all the fixed components above the jaws in the accelerator head (Deng *et al* 2000). What we need to consider for routine dose calculations are the jaws, wedges, blocks, compensators, MLC and bolus. For electron beams our multiple-source model covers all the components down to the lowest scraper of the applicator (Jiang *et al* 2000a). Only the electron cutout and bolus need to be considered in MCDOSE.

The x and y jaws are modelled as two pairs. The inner surface of each jaw focuses to the target. The input parameters are $x1$, $x2$, $y1$, $y2$ and the material for the jaws. Here $x1$, $x2$, $y1$, $y2$ specify the locations of the inner edges of the jaw bars. They correspond to the field size at 100 cm SSD. A schematic diagram for the jaws is shown in figure 1(*a*).
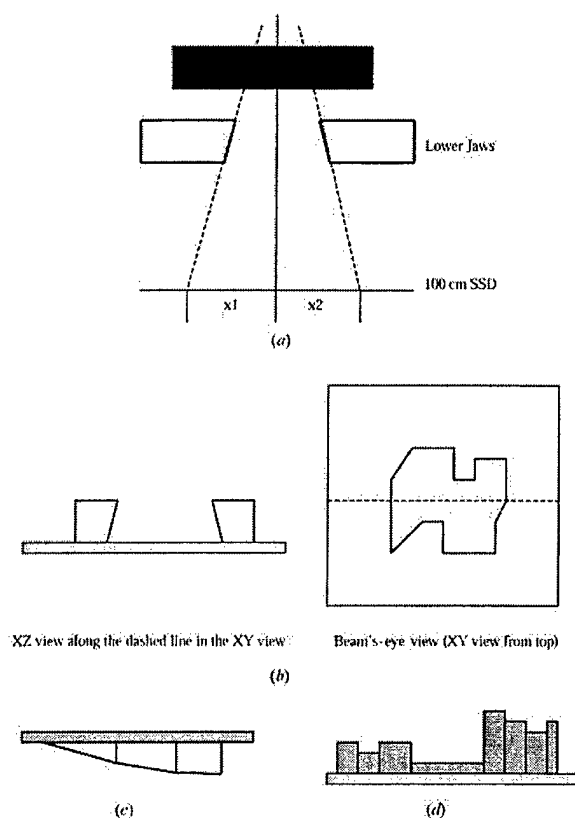
Figure 1. Schematic diagram of the beam modifiers simulated in MCDOSE. (*a*) *X* and *Y* jaws. (*b*) Photon beam block with tray. (*c*) Wedge and tray. (*d*) Compensator and tray.

To simulate the treatment block and the tray, the location, thickness and material of the block and the tray are required. The location is defined as the distance to the isocentre from the bottom surface of the block tray. The user also needs to specify the opening by the coordinates of the vertices that are projected at 100 cm SSD. The planes defining the inner surfaces of the opening are all angled with respect to the Z-axis towards the target as a single focus point. The block opening can be of any shape. The user needs to input the points continuously around the perimeter of the opening. The beam's eye view and $X–Z$ view of the block and tray are shown in figure 1(*b*).

Wedges can be simulated by MCDOSE using the geometry information about the orientation, location, material and the two-dimensional point coordinates to specify its shape (see figure 1(*c*)). Full simulation of the particle transport is performed. This approach is similar to the wedge definition for conventional dose calculation algorithms, except for one important point. For the Monte Carlo approach, the user enters the exact wedge specifications without any modifications or adjustments in the parameters so that the final dose calculation matches the measured dose profiles of the wedge under consideration. Thus, in our Monte Carlo approach, the physical transport of particles in the beam modifiers and the

reproduction of the phase space must be accurate to obtain good agreement with measured results.

The compensator including the tray can be simulated by MCDOSE. The location, material and the tray thickness are required. The compensator is divided into different bins in two directions. The coordinates and thickness for each bin (a pixel) are required. An X–Z view of the compensator and tray is shown in figure 1(d). This module can also be used as an MLC after setting the tray material to air.

An electron cutout is simulated in a way similar to a photon block except that it does not have a tray. The option to have a diverging or straight and parallel inner planes to define the opening is considered for different clinical applications. The location, material and coordinates of each vertex to specify the opening are required.

The bolus is simulated by adding an extra layer of material to the patient's geometry (outside the patient external contour) according to its material and thickness.

2.2. Simulation of beam modifiers by EGS4/BEAM

In order to validate the code for beam modifier simulation in MCDOSE, EGS4/BEAM was used to simulate block, wedge, compensator and electron cutout. The simulations started with the phase space above the jaws. No variance reduction techniques were used in these simulations. The cut-off energy of electron and photon were set to be 700 keV and 10 keV (total energy). After the phase space data were obtained below the modifiers, DOSXYZ was used to carry out the dose calculation. Comparison between them can prove that our implementation for the simulation of beam modifier is right.

Two component modules, BLOCK and SLABS, were used to simulate the photon blocks and the trays. To simulate the wedge, the left bars of two or more pairs of JAWS were piled up to match the shape. The component modules MLC and SLABS were used to simulate the compensators and trays. The component BLOCK was used to simulate an electron cutout with the phase space above the last scraper as source input. Five subregions were used to specify a butterfly shape for the opening that was simulated for an electron cutout in this paper. The phase space data were scored below the modifiers. Then dose calculations were performed using DOSXYZ in a water phantom.

2.3. Variance reduction techniques and dose calculation details

The goal of MCDOSE is to perform quick and accurate dose calculation for radiation therapy treatment planning. Several variance reduction techniques have been implemented in MCDOSE to speed up the calculation without losing accuracy. These techniques include electron range and region rejection, photon interaction forcing, particle splitting, Russian roulette (Bielajew and Rogers 1988) and electron track repeating (Kawrakow *et al* 1996, Keall and Hoban 1996b). To speed up the simulation in beam modifiers, the electron region rejection technique was applied to the electrons that make little contribution to the dose. For example, when we transport particles in jaws and blocks, we have an option to transport electrons only in a margin around the opening. Variable global cut-off energy (ECUT) has been applied to different regions. The techniques of photon interaction forcing, splitting and Russian roulette are well known and are implemented in some codes, such as BEAM/EGS4 system. They were well described by Bielajew and Rogers (1988) and Rogers *et al* (1995). Electron track repeating is similar to a technique called correlated sampling (Ma and Nahum 1993), in which particle tracks were repeated in different locations or geometries to improve computation efficiency. It was described in great detail by Kawrakow *et al* (1996) and Keall and Hoban (1996b). The main
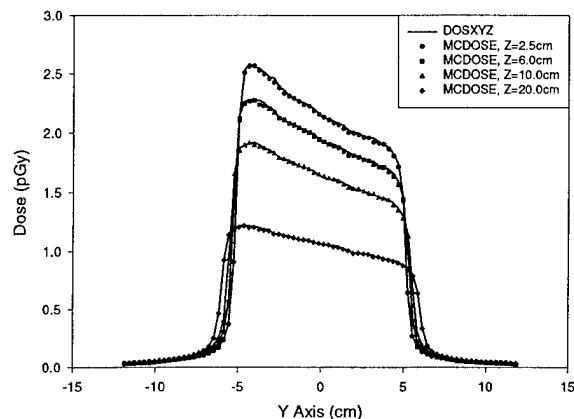
Figure 2. Comparisons of the lateral dose profiles at different depths in a water phantom between MCDOSE and BEAM/DOSXYZ. A 45° wedge were simulated for a 15 MV photon beam, the field size was 10 cm × 10 cm defined at 100 cm SSD.

idea is to simulate an electron in a standard phantom such as in water or tissue, recording all the information of the electron transport tracks including the step length, direction, energy deposition, type of collision and generated particles for each step, then repeat the tracks for other electrons with the same energy starting from a different location in the patient. The initial direction for each electron may be different. The length of every step in the electron track is inversely proportional to the material density at that location. Stopping power ratio and scattering power ratio for different materials need to be considered to scale the path lengths and multiple scattering angles. This technique saves the sampling time for multiple scattering and collision for all the repeated electrons but not for the initial one. How many times to repeat the tracks depends on the problem. The number may affect the final efficiency. Our goal was to integrate this technique efficiently with other techniques mentioned above to produce a fast Monte Carlo code. For example, when photons go into the phantom, they are split and forced to have same interactions at different locations. Many electrons are generated and their tracks are repeated at these locations. So time is saved because we do not perform initial simulation for all the electrons. Russian roulette is applied to reduce the number of scattering photons.

To ensure the accuracy of the dose calculation with MCDOSE, specially designed inhomogeneous phantoms, such as layered-lung or layered-bone phantoms, are used. The dose distributions (depth dose curves and lateral dose profiles) calculated by MCDOSE and DOSXYZ for different photon beams and electron beams are compared. DOSXYZ was selected for comparison with MCDOSE because it has already been tested thoroughly and it is also an EGS4 user code. Agreement between MCDOSE and DOSXYZ means that the beam modifier implementation in MCDOSE is correct and the application of variance reduction techniques does not affect the accuracy. Since DOSXYZ has been well benchmarked by other investigators and our previous work (Rogers *et al* 1995, Kapur *et al* 1998, Ma 1998, Zhang *et al* 1999, Ma *et al* 1999a, 2000a), it is not necessary to compare all the MCDOSE results with measurements. In this work, both monoenergetic photon beams and realistic clinical beams of Varian 2300C/D are studied. The goal for use of monoenergetic photon beams is to make sure that the code works well for monoenergetic beams (therefore it should also work
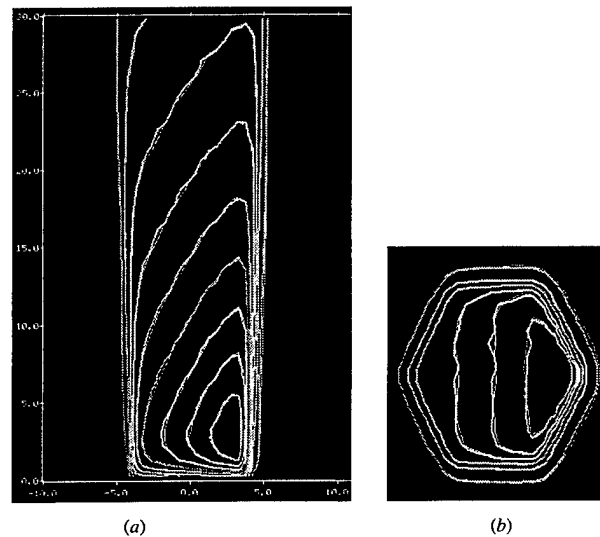
(a)   (b)

Figure 3. Dose distributions in a water phantom calculated by MCDOSE (thin curve) and BEAM/DOSXYZ (thick curve) for a 10 cm × 10 cm field of a 15 MV photon beam. The beam was modified by a hexagonal block and a 60° wedge. (a) The isodose distribution in the X–Z plane through the central axis (beams come from the bottom). (b) The isodose distribution in the X–Y plane at a depth of 3.5 cm.

for polyenergetic beams). This test was done thoroughly in the energy range of interest for dosimetry with an interval of 1 MeV.

3. Results

3.1. Validation of beam modifiers

3.1.1. A 45° wedge. Figure 2 shows the lateral dose profiles at different depths in a water phantom calculated using MCDOSE and BEAM/DOSXYZ for a 45° wedge. Lead was used as the wedge material. The field size was set to 10 cm × 10 cm at 100 cm SSD. The voxel size in the water phantom was 1.0 cm × 0.3 cm × 0.5 cm. A 15 MV photon beam from a Varian Clinac 2300C/D machine was used as source input with phase space scored above the jaws. The comparison calculations were performed under the same conditions. The agreement between the results of MCDOSE and BEAM/DOSXYZ is within 1% of the maximum dose. The CPU time comparison between MCDOSE and BEAM/DOSXYZ is shown in table 1. MCDOSE is about 16 times faster than BEAM/DOSXYZ for this simulation.

3.1.2. A hexagonal block and a 60° wedge. Figure 3 shows the dose distributions calculated by MCDOSE and BEAM/DOSXYZ in a water phantom with a hexagonal block and a 60° wedge for a 10 cm × 10 cm field of a 15 MV photon beam. The block was made of Cerrobend and its thickness was 7.7 cm. The block tray was made of PMMA and its thickness was 0.7 cm. The wedge was made of lead. The voxel size in the water phantom was 0.5 cm × 0.5 cm × 0.5 cm. Figure 3(a) shows the isodose distribution in the X–Z plane through the central axis and figure 3(b) shows the isodose distribution in the X–Y plane at a depth of 3.5 cm. The difference between the results of MCDOSE and BEAM/DOSXYZ is within 1% of the maximum dose.
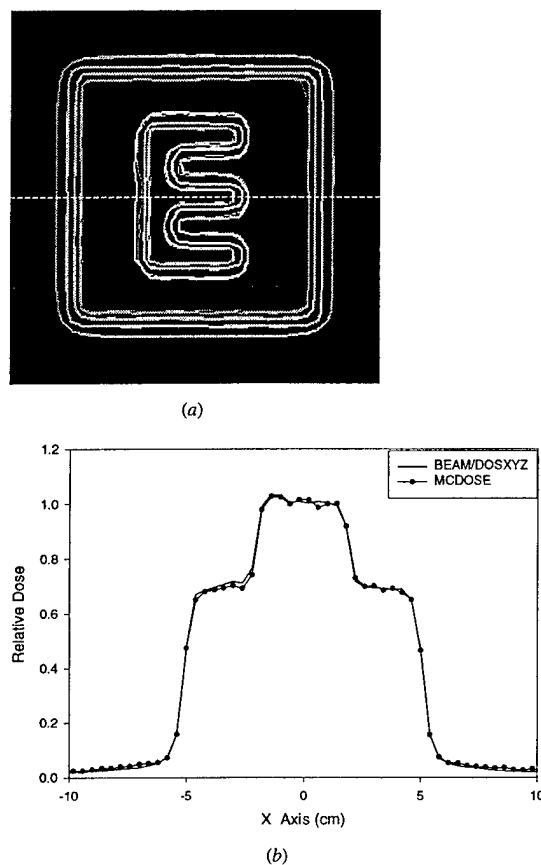
(a)

(b)

Figure 4. (a) The isodose distributions in XY view at a depth of 2.5 cm in a water phantom for a modified 10 cm × 10 cm 15 MV photon beam using a specially designed compensator. The thick curve is the simulation result of BEAM/DOSXYZ. The thin curve is the result of MCDOSE. (b) The lateral dose profile along the dashed line in (a). The curve with symbols in (b) is the result of MCDOSE.

Table 1. The CPU time (hours) required by MCDOSE and BEAM/DOSXYZ for the beam modifier simulation investigated in this work on a Pentium III 450 MHz personal computer. The statistical uncertainties of the maximum doses are 1%.

	Modifier			
	45° wedge	60° wedge/block	E-shaped compensator	Butterfly-shaped electron cutout
BEAM + DOSXYZ	31.5 + 6.1	247.5 + 7.9	10.3 + 10.9	37.9 + 1.4
MCDOSE	2.3	13.0	5.3	2.5
Ratio	16.3	19.4	4.0	15.7

The CPU time needed by MCDOSE and BEAM/DOSXYZ is given in table 1. MCDOSE is about 19 times faster than BEAM/DOSXYZ for this simulation.
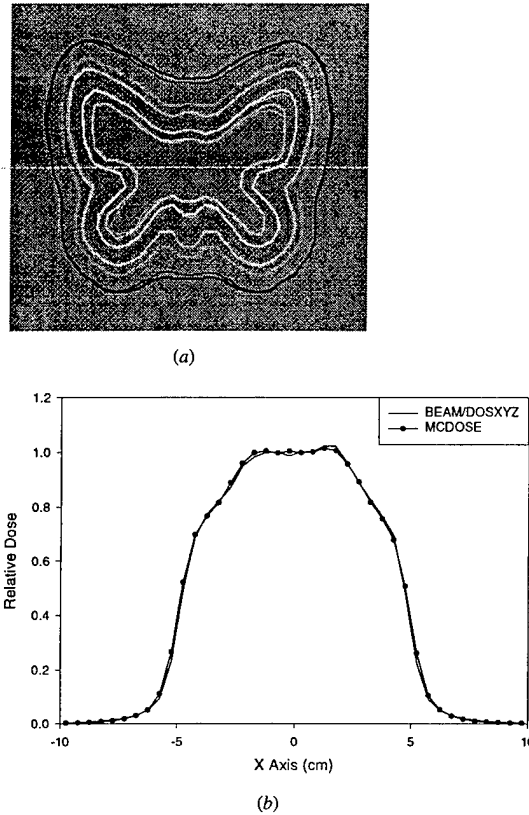
(a)

(b)

Figure 5. (a) is the isodose distributions in XY view at a depth of 2.25 cm in a water phantom for a modified 10 cm × 10 cm 12 MeV electron beam using an electron cutout with a butterfly-shaped opening. The thick curve is the simulation result of BEAM/DOSXYZ. The thin curve is the result of MCDOSE. (b) The lateral dose profile along the dashed line in (a). The curve with symbols in (b) is the result of MCDOSE.

3.1.3. Compensator. Figure 4 shows the E-shaped compensator isodose distributions (a) and lateral dose profiles (b) at a depth of 2.5 cm in the water phantom. They were calculated using MCDOSE and BEAM/DOSXYZ respectively. The compensator was made of copper. The thickness in the area of the compensator forming the 'E' shape was 0.5 cm and the thickness in the remaining area was 2 cm. The voxel size in the water phantom was 0.4 cm × 0.4 cm × 1.0 cm. Agreement (within 1%) can be observed from the comparison. In the penumbra regions, the separation between the results of MCDOSE and BEAM/DOSXYZ is within 1 mm. The CPU time needed by MCDOSE and BEAM/DOSXYZ is also shown in table 1. MCDOSE is about four times faster than BEAM/DOSXYZ for this simulation.

3.1.4. Electron cutout. Figure 5 shows the isodose distributions (a) and lateral dose profiles (b) in a water phantom calculated using BEAM/DOSXYZ and MCDOSE, for a 12 MeV realistic electron beam from a Varian 2100C machine with a butterfly-shaped cutout. The cutout was made of Cerrobend and its thickness was 1.4 cm. The voxel size in the water phantom
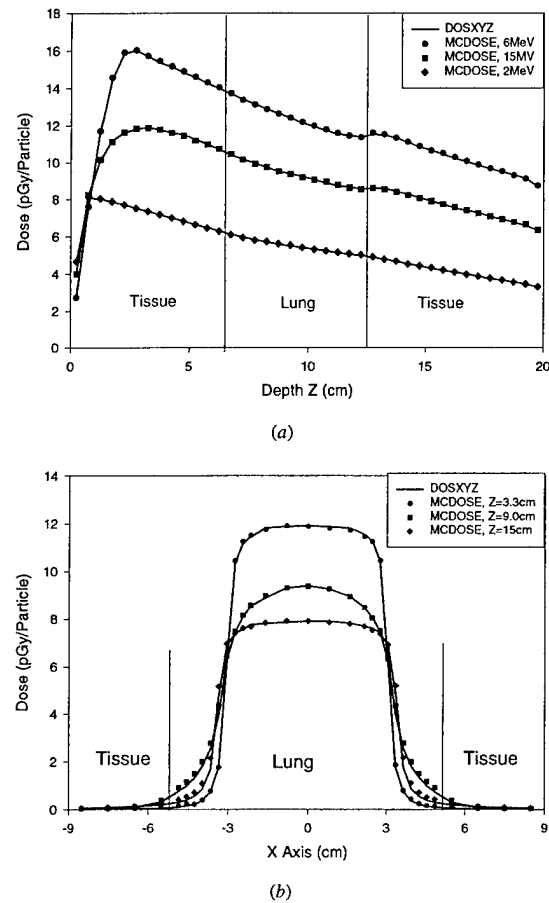
(a)

(b)

Figure 6. Dose distribution in a tissue–lung–tissue phantom calculated by DOSXYZ and MCDOSE for 6 MeV, 15 MV and 2 MeV photon beams with field size of 6 cm × 6 cm defined at 100 cm SSD. The material in the volume of −5.0 cm to 5.0 cm along the X direction, −2.0 cm to 2.0 cm along the Y direction and 7.0 cm to 12.5 cm along the Z direction is lung. (*a*) The depth dose curves along the central axis for the beams. (*b*) The lateral dose profiles along the X-axis at depths of 3.3 cm, 9.0 cm and 15.0 cm for the 15 MV photon beam.

was 0.5 cm × 0.5 cm × 0.3 cm. The phase space of an electron beam above the last scraper of a 10 cm × 10 cm applicator was used as the source input. Good agreement (within 1%) has been achieved between the results of MCDOSE and BEAM/DOSXYZ. In the penumbra regions, the separation between MCDOSE and BEAM/DOSXYZ is within 1 mm. The CPU time needed by MCDOSE and BEAM/DOSXYZ is shown in table 1. MCDOSE is about 16 times faster than BEAM/DOSXYZ for this simulation.

The electron beam cutout factors calculated using MCDOSE are compared with the published data in table 2. The published data were calculated using BEAM/DOSXYZ with full phase space input and measured by Kapur *et al* (1998). The difference between the MCDOSE data and those calculated with full phase space by DOSXYZ is within 1.0%. The differences
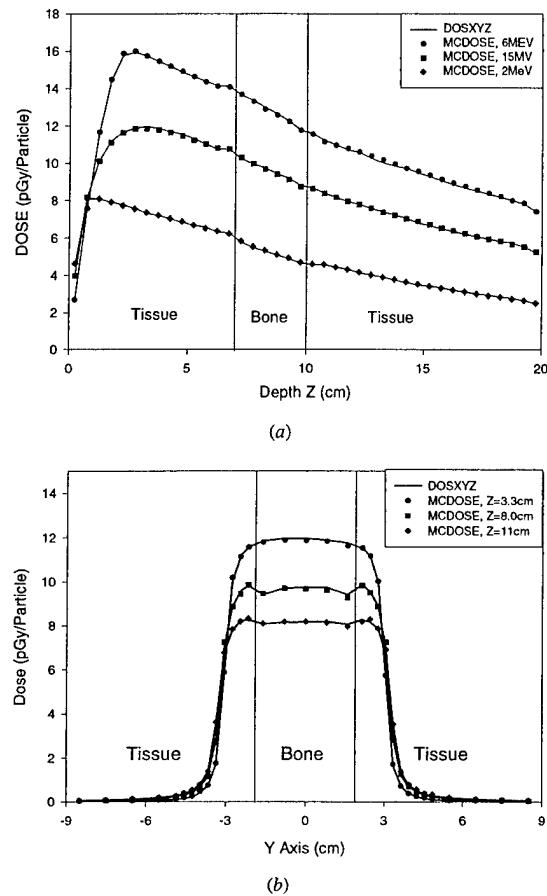
(a)

(b)

Figure 7. Dose distributions in a tissue–bone–tissue phantom calculated by DOSXYZ and MCDOSE for 6 MeV, 15 MV and 2 MeV photon beams with field size of 6 cm × 6 cm defined at 100 cm SSD. The material in the volume of −5.0 cm to 5.0 cm along the X direction, −2.0 cm to 2.0 cm along the Y direction and 7.0 cm to 10.0 cm along the Z direction is bone. (*a*) The depth dose curve along the central axis for the beams. (*b*) The lateral dose profiles along the Y axis at depths of 3.3 cm, 8.0 cm and 11.0 cm for the 15 MV photon beam.

in the cutout factors between MCDOSE data and measurement is less than 2% except for the cases of 20 MeV electron beams with 3 cm × 3 cm and 4 cm × 4 cm inserts.

3.2. Validation of dose distribution in heterogeneous phantoms

To test the accuracy of the dose distribution calculated using MCDOSE with the variance reduction techniques, comparisons are made with the results of DOSXYZ. Each example has been calculated with a source–surface distance of 100 cm and field size of 6 cm × 6 cm. The global electron cut-off energy (ECUT) was set to 700 keV and photon cut-off energy (PCUT) was set to 10 keV in MCDOSE and DOSXYZ. The maximum fractional energy loss per electron step (ESTEPE) was limited to 4% for both codes. The material compositions and
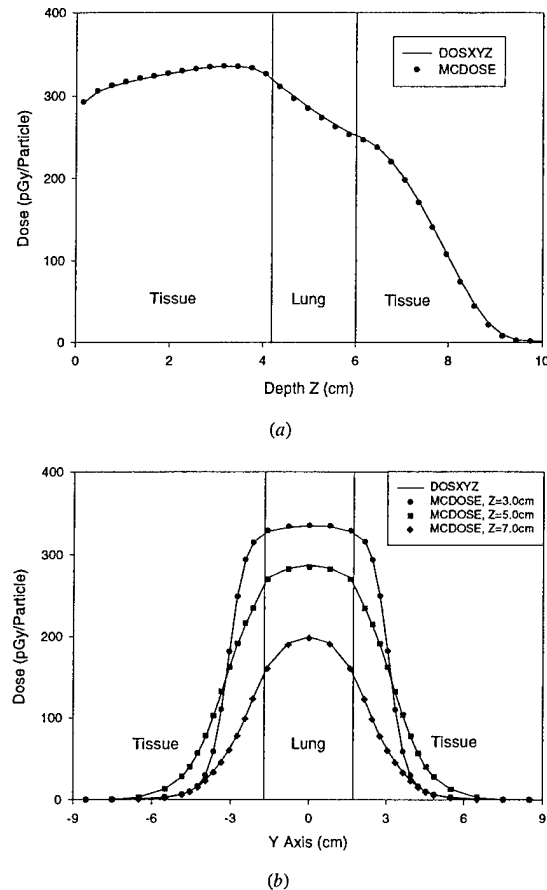
Figure 8. Dose distributions in a tissue–lung–tissue phantom calculated by DOSXYZ and MCDOSE for a 15 MeV electron beam with field size 6 cm × 6 cm. The material in the volume of −5.0 cm to 5.0 cm along the X direction, −2.0 cm to 2.0 cm along Y direction and 4.2 cm to 6.0 cm along the Z direction is lung. (a) The depth dose curve along the central axis. (b) The lateral dose profiles along the Y-axis at depths of 3.0 cm, 5.0 cm and 7.0 cm.

densities are taken from ICRU (1992). Monoenergetic point sources and phase space files for a 15 MV photon beam of a Varian Clinac 2300C/D linear accelerator were used. Since dose per incident fluence is calculated, absolute dose comparisons are made between MCDOSE and DOSXYZ.

3.2.1. Photon beams. Figure 6(a) shows the depth dose curves along the central axis for 6 MeV and 2 MeV monoenergetic photon beams calculated by DOSXYZ and MCDOSE in a tissue phantom with 3D lung inhomogeneity. At depths from 7 cm to 12.5 cm, the phantom contains a 10 cm × 4 cm slab of lung in the centre. The depth dose curves for a realistic 15 MV photon beam from a Varian Clinac 2300C/D accelerator calculated by DOSXYZ and MCDOSE in the same phantom are also shown in figure 6(a) and the lateral dose profiles at
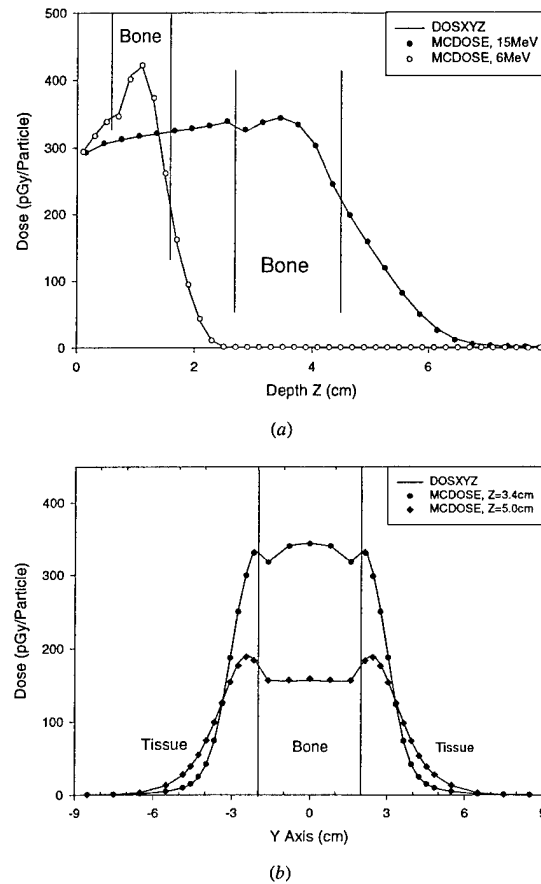
Figure 9. Dose distribution in tissue–bone–tissue phantoms calculated by DOSXYZ and MCDOSE for 15 MeV and 6 MeV electron beams with field size 6 cm × 6 cm. For the 15 MeV electron beam, the material in the volume of −5.0 cm to 5.0 cm along the *X* direction, −2.0 cm to 2.0 cm along the *Y* direction and 2.7 cm to 4.5 cm along the *Z* direction is bone. For the 6 MeV electron beam, the material in the volume of −5.0 cm to 5.0 cm along the *X* direction, −2.0 cm to 2.0 cm along the *Y* direction and 0.6 cm to 1.6 cm along the *Z* direction is bone. (*a*) The depth dose curves along the central axis for two beams. (*b*) The lateral dose profiles along the *Y* axis at depths of 3.4 cm and 5.0 cm for the 15 MeV electron beam.

different depths are shown in figure 6(*b*). The phase space for a 15 MV photon beam was generated by BEAM and contains over 5 million particles. The 1σ statistical uncertainty on the dose values for these curves is less than 0.5%.

Dose calculations were also performed for photon beams in an inhomogeneous phantom containing tissue and bone. A 10 cm × 4 cm slab of bone was placed between 7 cm and 10 cm depth in the centre of the tissue phantom. Figure 7(*a*) shows the depth dose curves along the central axis for different photon beams. Figure 7(*b*) shows the lateral dose profiles at different depths for a 15 MV photon beam.

Figures 6 and 7 show good agreement in dose distributions between MCDOSE and DOSXYZ for different photon beams. The absolute doses calculated by these two codes

Table 2. The electron cutout factors for various square inserts in 10×10 cm^2 applicator for 6, 12 and 20 MeV beams calculated by MCDOSE and compared with the full phase space calculation by DOSXYZ and measurement of Kapur *et al* (1998). The values in the parentheses indicate the per cent difference between the MCDOSE calculated data and those measured or calculated with full phase space by DOSXYZ.

Energy (MeV)	Insert (cm × cm)	MCDOSE	Full phase space	Measurement
6	3 × 3	0.922	0.923 (−0.1%)	0.927 (−0.5%)
	4 × 4	0.983	0.982 (0.1%)	0.988 (−0.5%)
	8 × 8	1.009	1.005 (0.4%)	1.003 (0.6%)
12	3 × 3	0.930	0.930 (0.0%)	0.928 (0.2%)
	4 × 4	0.965	0.956 (0.9%)	0.963 (0.2%)
	8 × 8	0.999	1.002 (−0.3%)	0.991 (0.8%)
20	3 × 3	0.964	0.968 (−0.4%)	0.993 (−2.9%)
	4 × 4	0.989	0.993 (−0.4%)	1.011 (−2.2%)
	8 × 8	0.999	0.993 (0.6%)	1.004 (−0.5%)

in tissue, lung, bone, even at the interface between tissue and bone and tissue and lung agree to within 1% of the maximum dose. Further comparisons of dose calculations for monoenergetic photon beams from 1 MeV to 20 MeV, and also for 6 MV and 10 MV photon beams were performed. Similar agreement between MCDOSE and DOSXYZ was achieved. In most cases, the differences were within the 1σ statistical uncertainty of 1%.

3.2.2. Electron beams. We also performed dose calculations for monoenergetic point source electron beams with field size 6 cm × 6 cm. The depth dose curves of a 15 MeV electron beam calculated by MCDOSE and DOSXYZ in a tissue–lung–tissue phantom are shown in figure 8(a). The lung material was at a depth from 4 to 6 cm. Figure 8(b) shows the lateral dose profiles at different depths in the phantom. At a depth from 4.2 to 6.0 cm, the lung material was from −5 cm to 5 cm in the X direction and from −2 cm to 2 cm in the Y direction. The remaining volume was tissue. The difference between the simulation results of MCDOSE and DOSXYZ is within 1% of the maximum dose.

The depth dose curves and lateral dose profiles at different depths for a 15 MeV electron point source beam in a tissue–bone–tissue phantom are shown in figures 9(a) and (b). At a depth from 2.7 to 4.5 cm, there was a 10 cm × 4 cm slab of bone in the centre surrounded by tissue. The depth dose curve for a 6 MeV electron beam in a tissue–bone–tissue phantom is also shown in figure 9(a). The bone material was at a depth from 0.6 to 1.6 cm. The difference between the simulation results of MCDOSE and DOSXYZ is within 1% of the maximum dose.

3.2.3. CPU time comparison. The CPU times required by MCDOSE and DOSXYZ for dose calculations shown in figures 6 and 9 are listed in table 3 for different photon and electron beams. The calculations were performed on a Pentium III 450 MHz PC. The statistical uncertainty of the maximum dose is 1%. The ratios in the table are the speed-up factors of MCDOSE compared with DOSXYZ for each beam. In general MCDOSE is 20–50 times faster than DOSXYZ for photon beams and 5–10 times faster than DOSXYZ for electron beams.

4. Summary

A new Monte Carlo dose calculation tool has been developed and validated for clinical dose calculation. The main features of MCDOSE include electron and photon beam reconstruction

Table 3. The CPU time (hours) required by MCDOSE and DOSXYZ for the dose calculations shown in figures 6 and 9 on a Pentium III 450 MHz personal computer. The statistical uncertainties of the maximum doses are 1%.

	Beam				
	2 MeV photon	6 MeV photon	15 MV photon	6 MeV electron	15 MeV electron
DOSXYZ	9.44	2.95	4.86	0.78	0.94
MCDOSE	0.25	0.074	0.098	0.08	0.17
Ratio	37.7	39.8	49.6	9.8	5.6

by source models, simulation of beam modifiers together with the patient geometry for dose calculation and application of variance reduction techniques.

Comparisons of dose distribution with wedges, blocks, compensator and electron cutout between MCDOSE and BEAM/DOSXYZ demonstrated that dose calculation with modifiers in MCDOSE is accurate, convenient and efficient. To compare MCDOSE and DOSXYZ dose distributions, 3D heterogeneous phantoms containing lung and bone were used. Excellent agreement between the MCDOSE and DOSXYZ results has been obtained for both photon and electron beams of different energies. Comparing with DOSXYZ, the MCDOSE code runs generally 20–50 times faster for the photon beams and 5–10 times faster for electron beams investigated in this work without beam modifiers.

Acknowledgments

References

Andreo P 1991 Monte Carlo technique in medical physics *Phys. Med. Biol.* **36** 861–920
Berger M J and Seltzer S M 1973 ETRAN, Monte Carlo code system for electron and photon transport through extended media *Documentation for RSIC Computer Package CCC-107* (Oak Ridge, TN: Oak Ridge National Laboratory)
Bielajew A F and Rogers D W O 1987 PRESTA: the parameter reduced electron-step transport algorithm for electron Monte Carlo transport *Nucl. Instrum. Methods Phys. Res.* B **18** 165–81
——1988 Variance-reduction techniques *Proc. Int. School of Radiation Damage and Protection Eighth Course: Monte Carlo Transport of Electrons and Photons below 50 MeV* ed T M Jenkins, W R Nelson and A Rindi (New York: Plenum) pp 407–19
DeMarco J J, Solberg T D and Smathers J B 1998 A CT-based Monte Carlo simulation tool for dosimetry planning and analysis *Med. Phys.* **25** 1–11
Deng J, Jiang S B, Kapur A, Li J S, Pawlicki T and Ma C-M 2000 Photon beam characterization and modelling for Monte Carlo treatment planning *Phys. Med. Biol.* **45** 411–27
Faddegon B A, Balogh J, Mackenzie R and Scora D 1998 Clinical considerations of Monte Carlo for electron radiotherapy treatment planning *Radiat. Phys. Chem.* **53** 217–28
Fippel M 1999 Fast Monte Carlo dose calculation for photon beams based on the VMC electron algorithm *Med. Phys.* **26** 1466–75
Hartmann-Siantar C L *et al* 1997 Lawrence Livemore National Laboratory's PEREGRINE Project *Proc. 12th Int. Conf. on the Use of Computers in Radiation Therapy (Salt Lake City, UT)* (Madison, WI: Medical Physics Publishing) pp 19–22

Hendricks J S 1994 A Monte Carlo code for particle transport *Los Alamos Scientific Laboratory Report* **22** 30–43

ICRU 1992 Photon, electron, proton and neutron interaction data for body tissues *ICRU Report* 46 (Bethesda, MD: ICRU)

Jeraj R and Keall P 1999 Monte Carlo-based inverse treatment planning *Phys. Med. Biol.* **44** 1885–96

Jiang S B, Boyer A L and Ma C-M 2000b Modeling the extrafocal radiation and monitor chamber backscatter for photon beam dose calculation *Med. Phys.* accepted

Jiang S B, Kapur A and Ma C-M 2000a Electron beam modelling and commissioning for Monte Carlo treatment planning *Med. Phys.* **27** 180–91

Kapur A, Ma C-M, Mok E C, Findley D O and Boyer A L 1998 Monte Carlo calculation of electron beam output factors for a medical linear accelerator *Phys. Med. Biol.* **43** 3479–94

Kawrakow I, Fippel M and Friedrich K 1996 3D electron dose calculation using a voxel based Monte Carlo algorithm (VMC) *Med. Phys.* **23** 445–57

Keall P J and Hoban P W 1996a Super-Monte Carlo: a 3D electron beam dose calculation algorithm *Med. Phys.* **23** 2023–34

——1996b Superposition dose calculation incorporating Monte Carlo generated electron track kernels *Med. Phys.* **23** 479–85

Libby B, Siebers J and Mohan R 1998 Systematic analysis of Monte Carlo generating beam weights *Med. Phys.* **23** 965–71

Ma C-M 1998 Characterization of computer simulated radiotherapy beams for Monte Carlo treatment planning *Radiat. Phys. Chem.* **53** 329–44

Ma C-M, Faddegon B A, Rogers D W O and Mackie T R 1997 Accurate characterization of Monte Carlo calculated electron beams for radio-therapy *Med. Phys.* **24** 401–16

Ma C-M, Li J S, Pawlicki T, Jiang S B and Deng J 2000c MCDOSE: a Monte Carlo dose calculation tool for radiation therapy treatment planning *Proc. 13th Int. Conf. on the Use of Computers in Radiation Therapy (Heidelberg, Germany)* (Berlin: Springer) pp 123–5

Ma C-M, Mok E, Kapur A and Findley D 1997 Improvement of small-field electron beam dosimetry by Monte Carlo simulations *Proc. 12th Int. Conf. on the Use of Computers in Radiation Therapy (Salt Lake City, UT)* (Madison, WI: Medical Physics Publishing) pp 159–62

Ma C-M, Mok E, Kapur A, Pawlicki T, Findley D, Brain S, Forster K and Boyer A L 1999a Clinical implementation of a Monte Carlo treatment planning system *Med. Phys.* **26** 2133–43

Ma C-M and Nahum A E 1993 Calculation of absorbed dose ratios using correlated Monte Carlo sampling *Med. Phys.* **20** 1189–99

Ma C-M, Pawlicki T, Jiang S B, Li J S, Deng J, Mok E, Kapur A, Xing L, Ma L and Boyer A L 2000a Monte Carlo verification of IMRT dose distributions from a commercial treatment planning optimization system *Phys. Med. Biol.* **45** 2483–95

Ma C-M, Pawlicki T, Lee M C, Jiang S B, Li J S, Deng J, Yi B, Mok E and Boyer A L 2000b Energy- and intensity-modulated electron beams for radiotherapy *Phys. Med. Biol.* **45** 2293–311

Ma C-M, Pawlicki T, Li J S, Jiang S B, Deng J, Kapur A, Mok E, Luxton G and Boyer A L 1999b MCDOSE—A dose calculation tool for radiotherapy treatment planning (abstract) *Med. Phys.* **26** 1148

Ma C-M, Reckwerdt P, Holmes M, Rogers D W O, Geiser B and Walters B 1995 DOSXYZ users manual *NRCC Report* PIRS-0509B

Mackie T R 1990 *Dosimetry of Ionizing Radiation* vol 3, ed K Kase, B Bjarngard and F H Attix (New York: Academic) pp 541–620

Mackie T R *et al* 1994 The OMEGA project: comparison among EGS4 electron beam simulations, 3D Fermi-Eyges calculations, and dose measurements *Proc. 11th Int. Conf. on the Use of Computers in Radiation Therapy (Manchester, UK)* pp 152–3

Mohan R 1997 Why Monte Carlo? *Proc. 12th Int. Conf. on the Use of Computers in Radiation Therapy (Salt Lake City, UT)* (Madison,WI: Medical Physics Publishing) pp 16–18

Mubata C D, Nahum A E, Rosenberg I and Bielajew A F 1998 Optimization of Monte Carlo simulation in external-beam treatment planning *Med. Phys.* **25** A185

Nahum A E 1997 Conformal therapy needs Monte Carlo dose computation *Proc. Challenges in Conformal Radiotherapy* (Nice: European Society for Therapeutic Radiology and Oncology) pp 1–11

Nelson W R, Hirayama H and Rogers D W O 1985 The EGS4 code system *Stanford Linear Accelerator Center Report* SLAC-265 (Stanford, CA: SLAC)

Neuenschwander H and Born E 1992 A macro Monte Carlo method for electron beam dose calculation *Phys. Med. Biol.* **37** 107–25

Neuenschwander H, Mackie T R and Reckwerdt P J 1995 MMC: a high performance Monte Carlo code for electron beam treatment planning *Phys. Med. Biol.* **40** 543

Pawlicki T, Jiang S B, Deng J, Li J S and Ma C-M 1999 Monte Carlo calculated beamlets for photon beam inverse planning (abstract) *Med. Phys.* **26** 1064–5

Rogers D W O 1984a Fluence to dose equivalent conversion factors calculated with EGS3 for electrons from 100 keV to 20 GeV and photons from 11 keV to 20 GeV *Health Phys.* **46** 891

——1984b Low energy electron transport with EGS *Nucl. Instrum. Methods* A **227** 535

Rogers D W O and Bielajew A F 1984 The use of EGS for Monte Carlo calculations in medical physics *NRCC Report* PXNR-2692 (Ottawa: NRCC)

——1986 Difference in electron depth-dose curve calculated with EGS and ETRAN and improved energy-range relationships *Med. Phys.* **13** 687–94

——1990 *Dosimetry of Ionizing Radiation* vol 3, ed K Kase, B Bjarngard and F H Attix (New York: Academic) pp 427–539

Rogers D W O, Bielajew A F, Mackie T R and Kubsad S S 1990 The OMEGA project: treatment planning for electron-beam radiotherapy using Monte Carlo techniques *Phys. Med. Biol.* **35** 285

Rogers D W O, Faddegon B A, Ding G X, Ma C-M, We J and Mackie T R 1995 BEAM—a Monte Carlo code to simulate radiotherapy treatment units *Med. Phys.* **22** 503–24

Salvat F, Fernandez-Vera J M, Baro J and Sempau J 1996 *PENELOPE, An Algorithm and Computer Code for Monte Carlo Simulation of Electron-Photon Showers* (Barcelona: Informes Técnicos Ciemat)

Schach von Wittenau A E, Bergstrom P M and Cox L J 2000 Patient-dependent beam modifier physics in Monte Carlo photon dose calculations *Med. Phys.* **27** 935–47

Shortt K R, Ross C K, Bielajew A F and Rogers D W O 1986 Electron beam dose distributions near standard inhomogeneities *Phys. Med. Biol.* **31** 235–49

Siebers J, Libby B and Mohan R 1998 Trust, but verify: comparison of MCNP and BEAM Monte Carlo codes for generation of phase space distributions for a Varian 2100C *Med. Phys.* **25** A143

Walling R, Hartmann Siantar C, Albright N, Wieczorek D, Knapp D, Verhey L, May S and Moses E 1998 Clinical validation of the PEREGRINE Monte Carlo dose calculation system for photon beam teletherapy *Med. Phys.* **25** A128

Wang L, Chui C and Lovelock M A 1998 A patient-specific Monte Carlo dose-calculation method for photon beams *Med. Phys.* **25** 867–78

Zhang G G, Rogers D W O, Cygler J E and Mackie T R 1999 Monte Carlo investigation of electron beam output factors versus size of square cutout *Med. Phys.* **26** 743–50